Environmental and Experimental Botany 242 (2026) 106312

Contents lists available at ScienceDirect

Environmental and Experimental Botany

journal homepage: www.elsevier.com/locate/envexpbot

Research paper

Cysteine and glutathione improve mercury tolerance in rice by modulating cell wall binding, transport, and detoxification pathways

Yeon-Ok Kim [a,*], Dream Kim [a,b,c], Mahpara Safdar [a,b,c], Jangho Kim [a,b,c,**]

[a] Interdisciplinary Program in IT-Bio Convergence System, Chonnam National University, Gwangju 61186, Republic of Korea
[b] Department of Convergence Biosystems Engineering, Chonnam National University, Gwangju 61186, Republic of Korea
[c] Department of Rural and Biosystems Engineering, Chonnam National University, Gwangju 61186, Republic of Korea

ARTICLE INFO

Keywords:
Mercury
Cysteine
Glutathione
ABC transporter
Cell wall

ABSTRACT

Mercury (Hg), a highly toxic element, poses significant risks to plant growth and human health. This study investigated the mechanisms of Hg accumulation and tolerance by exogenous cysteine (Cys) and glutathione (GSH) in rice. Here, we showed that exogenous Cys and GSH significantly enhanced Hg tolerance in rice but exhibited contrasting effects on Hg accumulation. Exogenous Cys significantly increased Hg accumulation in rice roots, primarily in the cell wall, while exogenous GSH decreased root Hg accumulation. Exogenous Cys significantly increased the expression of cell wall biosynthesis genes, particularly those involved in lignin synthesis, resulting in greater lignin accumulation in epidermis, exodermis, and stele, which correlated with increased Hg binding to the cell wall. In addition, exogenous Cys significantly upregulated several ABC transporters, particularly OsABCGs and OsABCCs, suggesting their possible involvement in Hg transport and vacuolar sequestration. In the process of cellular Hg detoxification, GSH upregulated aquaporin to maintain membrane function and water balance, Cys primarily activated peroxidase-mediated H_2O_2 scavenging. Taken together, these findings highlight novel candidate genes involved in Hg cell wall binding, transport, and detoxification, regulated by Cys and GSH, offering insights for enhancing our understanding of the molecular mechanisms underlying Hg accumulation and tolerance. Furthermore, this study provides new insights into thiol-mediated Hg tolerance and offers potential strategies for reducing Hg accumulation in crops.

Introduction

Mercury (Hg) is a highly toxic pollutant originating from both natural processes and human activities such as fossil fuel combustion, waste incineration, and mining. Due to its extreme persistence in the environment, Hg readily accumulates in plants, posing a serious threat to crop productivity and food safety (Natasha et al., 2020; Tang et al., 2020). Given that rice (*Oryza sativa* L.) is one of the most widely cultivated food crops globally, mitigating Hg accumulation and toxicity in rice is critical for ensuring both agricultural productivity and human health. Hg strongly binds to the sulfhydryl (–SH) groups of proteins and other biomolecules, interfering with cellular metabolic processes such as enzyme activity, water transport, nutrient homeostasis, photosynthesis, and mitochondrial metabolism, ultimately leading to cell damage and growth inhibition in plants (Ajsuvakova et al., 2020; Natasha et al., 2020; Patra and Sharma, 2000).

Major plant non-protein thiols (NPTs) containing cysteine (Cys), such as glutathione (GSH), phytochelatins (PCs), and metallothioneins (MT), chelate Hg^{2+} ions through their Cys SH groups, converting Hg into less toxic forms and thereby reducing its harmful effects (Ajsuvakova et al., 2020; Dago et al., 2014; Kim et al., 2017, 2022; Manceau et al., 2019). As Cys serves as both a structural component of MTs and as the biosynthetic precursor of GSH—which subsequently serves as the substrate for PC synthesis—both Cys and GSH are considered essential for Hg accumulation and detoxification in plants. Studies have focused on investigating the direct roles of Cys and GSH through exogenous application studies under heavy metal (HM) stress. Although external application of Cys or GSH improves tolerance to Cd, Cr, and Pb in various plant species, their influence on metal uptake and accumulation differs among species (Terzi and Yıldız, 2021; Wang et al., 2011; Yildiz, Terzi., 2021; Zeng et al., 2012). Likewise, exogenous Cys and GSH enhances Hg tolerance in *Arabidopsis* but exert opposite effects on Hg

* Corresponding author.
** Corresponding author at: Interdisciplinary Program in IT-Bio Convergence System, Chonnam National University, Gwangju 61186, Republic of Korea.
E-mail addresses: kimyok@jnu.ac.kr (Y.-O. Kim), rain2000@jnu.ac.kr (J. Kim).

https://doi.org/10.1016/j.envexpbot.2026.106312
Received 10 October 2025; Received in revised form 6 January 2026; Accepted 9 January 2026
Available online 12 January 2026

accumulation (Kim et al., 2017, 2022), suggesting that Cys and GSH differentially modulate Hg uptake and cellular distribution. However, the underlying mechanisms remain largely unknown.

Several bacterial Hg transporters including *merA, merB, merC,* and *merT* have been identified and play crucial roles in Hg resistance, uptake, and accumulation in transgenic tobacco and *Arabidopsis* (Haque et al., 2010; Li et al., 2020; Uraguchi et al., 2019; Xu et al., 2017). In contrast, specific Hg transporters across the plant plasma membrane remain unidentified. Previous studies have highlighted the ability of thiol compounds to facilitate HM transport and sequestration. PCs bind to HMs and act as carriers for HM ions during long-distance transport from roots to shoots (Mendoza-Cózatl et al., 2010). PCs complexed with Cd, As, and Hg are transported into vacuoles via vacuolar transporters, such as *AtABCC1* and *AtABCC2* (Mendoza-Cózatl et al., 2010; Park et al., 2012; Song et al., 2010). GSH also forms HM complexes that are transported into vacuoles for sequestration (Roy et al., 2023). A recent study indicates that amino acid transporter *AtLHT1*, induced by exogenous Cys, may facilitate Hg uptake in the form of Hg–Cys complexes in *Arabidopsis* roots (Kim et al., 2022). As plant Hg transporters remain uncharacterized, exploring whether nonspecific transporters—including those modulated by Cys or GSH—contribute to Hg uptake could provide valuable insight into Hg accumulation mechanisms.

Intracellular Hg generates reactive oxygen species (ROS) and damages macromolecules, such as membrane components and proteins, resulting in mitochondrial dysfunction and impaired metabolic processes (Natasha et al., 2020; Vergilio et al., 2015; Zhou et al., 2007). The detoxification of excess ROS is mediated by an antioxidant system comprising enzymatic components—such as superoxide dismutase (SOD), peroxidase (POX), catalase (CAT), and glutathione reductase (GR)—and nonenzymatic antioxidants including GSH, ascorbic acid (AsA), and carotenoids, which collectively maintain cellular redox homeostasis (Foyer and Noctor, 2005; Mittler et al., 2004). Recent studies show that exogenous Cys enhances the expression and activity of antioxidant enzymes, including SOD, POD, CAT, and GR, under Co, Cr, Hg, and Cd stress in rapeseed, *Arabidopsis*, sweet basil, and maize (Aysin et al., 2020; Azarakhsh et al., 2015; Kim et al., 2022; Yildiz, Terzi., 2021). Similarly, exogenous GSH increases the activity of antioxidant enzymes and the levels of nonenzymatic antioxidants in As-treated rice and Cd-treated wheat (Jung et al., 2019; Li et al., 2021). However, evidence regarding how Cys and GSH modulate Hg-induced oxidative stress in rice is still limited, and understanding their regulatory effects on antioxidant gene expression could provide key insights into Hg tolerance mechanisms in this important crop.

Roots act as the primary barrier to Hg entry and predominantly retain Hg, thereby limiting its translocation to aerial tissues in many plant species (Ericksen and Gustin, 2004; Greger et al., 2005; Yuan et al., 2022). HM ions can also be adsorbed and immobilized in the cell wall to mitigate their toxic effects. The plant cell wall is a complex matrix composed mainly of cellulose, hemicellulose, lignin, and pectin (Voiniciuc et al., 2018; Yuan et al., 2022). Under HM stress, plants modify the biosynthesis of these polysaccharides to enhance metal binding capacity (Cheng et al., 2025). Lignin accumulation, commonly induced by Cd and Zn, strengthens the cell wall and reduces the movement of HMs from the apoplast into the cytoplasm (Dong et al., 2023; Kanwal et al., 2025). Therefore, elucidating the mechanisms of Hg sequestration in the root cell wall is important for understanding plant tolerance. Although previous RNA-Seq studies have identified Hg-responsive genes in rice roots (Chen et al., 2012, 2014; Huang et al., 2022), the cellular mechanisms underlying Hg uptake, sequestration, and metabolic fate remain poorly defined. Moreover, no study has comprehensively examined how Cys and GSH influence Hg responses in rice roots, highlighting the need to clarify the molecular pathways involved. Thus, this study aims to (1) determine how exogenous Cys and GSH differentially affect Hg uptake and intracellular distribution in rice roots after 1 day of Hg exposure; (2) identify key genes and pathways involved in Hg transport, sequestration, and detoxification through transcriptomic analysis; and (3) elucidate the regulatory mechanisms of candidate genes, —including membrane transporters, cell wall-related genes, and antioxidant genes—involved in the Cys- and GSH-mediated responses to Hg stress.

Materials and methods

Plant materials and growth conditions

Rice (*Oryza sativa* L. japonica cv. Nipponbare) seeds were surface-sterilized with a 10 % sodium hypochlorite solution for 20 min and thoroughly rinsed with deionized water to remove residual sodium hypochlorite. Subsequently, the seeds were sown on half-strength Murashige and Skoog (1/2 MS) medium supplemented with varying concentrations of $HgCl_2$ (~200 μM) with Cys or GSH for evaluation of germination rates and seedling growth (denoted as Hg, Hg+Cys, or Hg+GSH). In preliminary experiments, rice seeds failed to germinate in the presence of 400 μM $HgCl_2$, so 200 μM $HgCl_2$ was used as the maximum concentration for phenotypic analysis. In addition, 50 μM Cys and GSH were selected based on preliminary dose-response experiments showing effective mitigation of Hg toxicity without causing independent phytotoxicity. To examine the effects of Cys and GSH on seedling growth under Hg stress, germinated seeds were transferred to 1/2 MS medium containing $HgCl_2$ (50 μM and 100 μM), with 50 μM Cys and GSH, and the plates were incubated in a vertical orientation. On the other hand, 2 weeks old rice seedlings were exposed to 5 nM, 50 nM, or 20 μM $HgCl_2$, with or without Cys or GSH, for 24 h and used for subsequent analyses. All experiments were conducted in triplicate.

Determination of Hg content

Hydroponically grown rice seedlings were exposed to different $HgCl_2$ concentrations (5 nM–20 μM), with Cys or GSH, for 24 h. Subsequently, the seedlings were thoroughly rinsed with deionized water and separated into roots and shoots. To isolate subcellular fractions (cell wall, cytoplasm, and organelles), fresh root tissue (1.0 g) was homogenized in 10 mL of pre-chilled 10 mL extraction buffer solution (0.25 M sucrose, 50 mM Tris-HCl (pH 7.5), 1 mM dithiothreitol). The homogenate was centrifuged at 3000 × g for 10 min at 4°C, and the resulting pellet was designated as the cell wall fraction. The supernatant was further centrifuged at 15,000 × g for 30 min at 4°C, yielding a pellet (organelle fraction) and a supernatant (cytoplasmic fraction), collectively referred to as the soluble fraction (Yang et al., 2018). Subsequently, the Hg content in each fraction was determined. All samples were dried at 80°C until completely dehydrated, and the Hg content was measured using a DMA-80 Direct Mercury Analyzer (Milestone, Sorisole, Italy). Standard reference material (SRM) MESS-3 (NRCC, National Research Council, Canada) was used for the calibration and validation of analytical methods.

Transmission electron microscopy analysis of subcellular Hg distribution

Root tips were harvested and prepared for transmission electron microscopy (TEM) analysis. The root tips were pre-fixed in a modified Karnovsky's fixative (mixture of 4 % paraformaldehyde and 2.5 % glutaraldehyde in 50 mmol/L phosphate buffer, pH 7.2), post-fixed in 2 % osmium tetroxide, and dehydrated through a graded acetone series (30 %, 50 %, 70 %, 80 %, 90 %, and 100 %). Subsequently, the samples were infiltrated and embedded in Spurr’s low-viscosity epoxy resin for polymerization. Ultrathin sections (70 nm) were cut using an MTX Powertome X ultramicrotome (RMC Products, Boeckeler Instruments, Egham, UK) with a diamond knife and stained with 3 % uranyl acetate and lead citrate. The sections were analyzed using a JEOL JEM-1400 transmission electron microscope (JEOL, Leica Microsystems Inc., Buffalo Grove, IL, USA) operated at 80 kV.

Fourier transform infrared (FTIR) spectral analysis

The dried rice roots were ground and analyzed via Fourier transform infrared (FTIR) (PerkinElmer Spectum 3) spectrometer. FTIR spectra were recorded in the range of 4000–400 cm^{-1} with a resolution of 4 cm^{-1} .

Assessment of cellular damage

To evaluate cell wall integrity using propidium iodide (PI) staining, rice roots were treated with 20 μM $HgCl_2$ in the presence of 50 μM Cys or GSH for 24 h and then incubated in 5 mg/L PI solution for 5 min. For fluorescence microscopy, the root samples were mounted on glass slides (1.0–1.2 mm thick) with long coverslips (22 × 50 mm, 0.16–0.19 mm thick). Samples were visualized using a Zeiss LSM 880 confocal microscope with a 40 × objective lens, a 488 nm excitation wavelength, and collecting emission at 496–577 nm. Hydrogen peroxide (H_2O_2) content was measured using the potassium iodide method, where H_2O_2 reacts with iodide to form iodine, which is quantified spectrophotometrically at 410 nm (Kim et al., (2017). To evaluate membrane damage using Evans blue staining, the roots of the 10-day-old rice seedlings, as previously described, were incubated in a 0.25 % (w/v) Evans blue solution for 10 min and rinsed thoroughly with deionized water. Subsequently, the extent of dye taken up by the cells was quantified by grinding the 10 stained roots in 1 % SDS and measuring the absorbance at 600 nm. Aldehydes that originated from LOOH in the roots were visualized with Schiff's reagent (Yamamoto et al., 2001). Roots were stained with Schiff's reagent (Wako Pure Chemical) for 10 min, rinsed with a freshly prepared sulfite solution (0.5 % [w/v] $K_2S_2O_5$ in 0.05 M HCl), and then kept in the sulfite solution and were instantly photographed.

Histochemical and content determination of lignin

The lignin content in rice roots was quantified according to the method of Jang and Lee (2020)) with a few modifications. The rice roots were ground with liquid nitrogen and freeze-dried. The dried samples (10 mg) were transferred into a centrifuge tube containing 95 % ethanol, thoroughly mixed, centrifuged at 5000*g* for 4 min, and rinsed with distilled water twice. The pellets were then dried at 60 °C, and digested in 25 % acetyl bromide (% v/v in glacial acetic acid) at 70 °C for 30 min, then added to 0.9 mL of 2 M NaOH to terminate the digestion. The samples were then mixed with 3 mL of acetic acid and 0.1 mL of 7.5 M hydroxylamine HCl and centrifuged at 4000 g for 10 min. The supernatant was diluted 10-fold with glacial acetic acid. The absorbance at 280 nm of each sample was measured. To determine lignin deposition in rice roots, the roots were sectioned into 100-μm-thick slices using a razor blade. The sections were stained with phloroglucinol-HCl solution (one volume of concentrated HCl mixed with two volumes of 3 % (w/v) phloroglucinol in ethanol) and photographed under Zeiss Stemi 2000C stereo-zoom microscope.

RNA extraction and RNA-Seq analysis

Total RNA was extracted from the treated roots using a Plant RNA Extraction Kit (Qiagen, Valencia, CA, USA) following the instructions of the manufacturer. Three biological replicates were performed *per each treatment*. RNA quality and concentration were evaluated using a Nanodrop ND-8000 spectrophotometer (Nanodrop Technologies, Inc., Wilmington, DE, USA) or agarose gel electrophoresis. Sequencing libraries were prepared from 3 μg of RNA using the Illumina TruSeq RNA Sample Preparation Kit v2 (Illumina, Inc., San Diego, CA, USA) and sequenced on an Illumina Hiseq2000 platform. The transcriptome was uploaded to NCBI Sequence Read Archive (accession number PRJNA820281).

Identification and clustering analysis of differentially expressed genes

Differentially expressed genes (DEGs) were identified from the sequencing data based on a fold change (FC) of $\geq$ 2 (significantly upregulated) or $\leq$ -2 (significantly downregulated), a false discovery rate (FDR) $\leq$ 0.01, and a read count $\geq$ 100 across samples. The FDR was calculated using DESeq to identify the threshold p-value for multiple testing corrections. Cluster analysis was conducted to assess the differential upregulation and downregulation of annotated transcripts between each treatment group. Significance thresholds were set at FDR $\leq$ 0.1, p < 0.05, and log2 FC $\geq \pm 2$. To visualize trends in gene expression, the $\log_2$-transformed, normalized count values of each gene were standardized to a mean of 0 and standard deviation of 1. A heatmap was generated using the *pheatmap* package in R. Commonly upregulated and downregulated DEGs were identified across treatments compared to the control using the Venny diagram (v2.1.0). Mean-centered, log-transformed fragments per kilobase of transcript per million mapped reads (FPKM) values were used to generate hierarchical clustering heatmaps in Cluster (version 3.0) and visualized using Java TreeView (version 3.0).

Gene ontology enrichment analysis

Gene Ontology (GO) enrichment analysis of DEGs was performed using AgriGO to identify significantly enriched GO terms. The reference gene list and GO annotations were extracted from the Rice Genome Annotation Project (RGAP) database. GO term distributions were visualized using in-house scripts based on UniProt annotations for DEGs. GO enrichment analysis was performed using the GOseq R package, applying a significance threshold of $P < 0.05$. DEGs were categorized into GO domains, cellular components, molecular functions, and biological processes.

Validation of differential gene expression using quantitative real-time polymerase chain reaction

To validate the RNA-Seq results, the expression of selected DEGs was evaluated using quantitative real-time PCR (qRT-PCR). Total RNA (200 ng) was analyzed using TOPreal ™ SYBR Green qPCR High-ROX PreMIX (Enzynomics) with gene-specific primers, listed in Tables S1, on a Rotor-Gene Q PCR cycler (Qiagen, Valencia, CA, USA). Ubiquitin 5 was used as an internal control.

Statistical Analysis

All experiments were performed three independent replicates. Values were shown as the means ± standard deviation (SD). Statistical significance was determined using one- or two-way analysis of variance (ANOVA) followed by Tukey's test ($p < 0.05$).

Results

Exogenous Cys and GSH enhance Hg tolerance in rice

Rice seed germination was inhibited in a dose-dependent manner across various Hg concentrations (0–200 μM $HgCl_2$) (Fig. 1A). However, significant recovery was observed after the application of Cys and GSH. No germination occurred until day 6 at 200 μM Hg, while exogenous Cys and GSH promoted germination starting from day 3. Consistent with germination trends, post-germination root growth was significantly reduced under Hg stress but increased by the application of Cys and GSH (Fig. 1A). When seeds that had germinated under normal conditions were transferred to MS medium containing various Hg concentrations (50 μM and 100 μM), exogenous Cys and GSH significantly alleviated the severe inhibition of seedling growth caused by Hg (Fig. 1B).

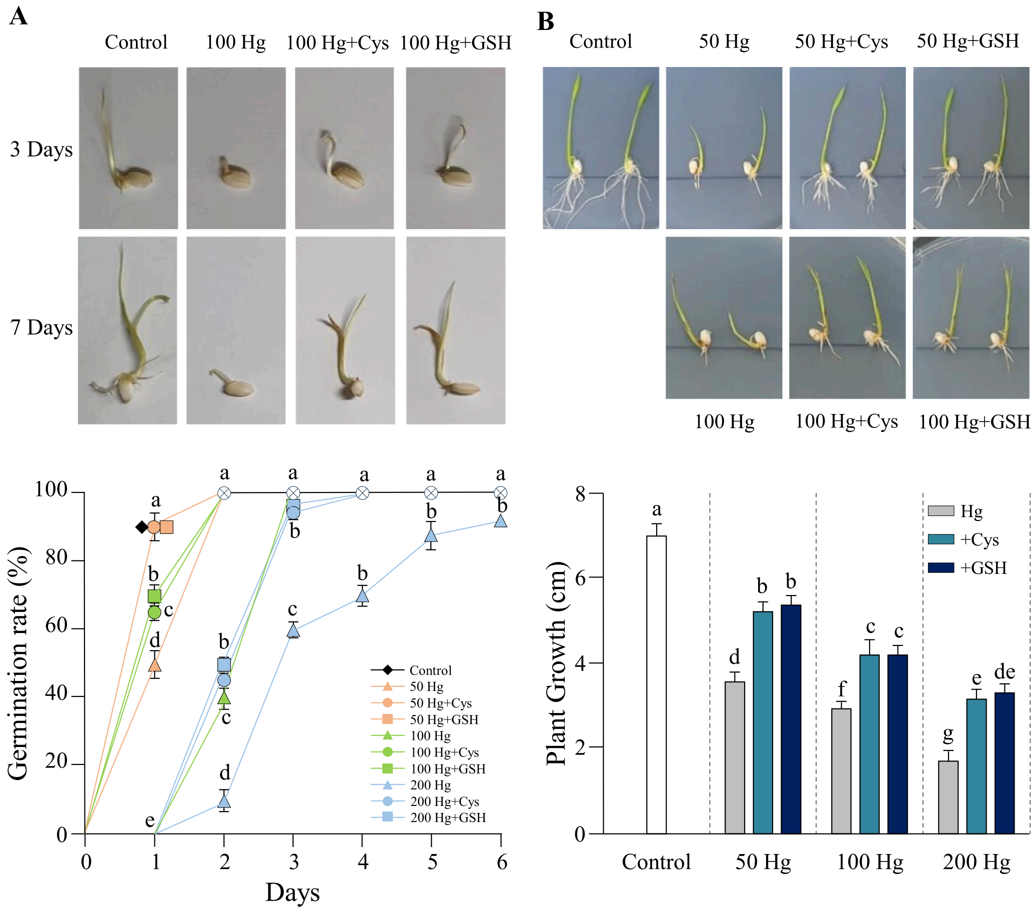

Fig. 1. Effects of exogenous Cys and GSH on rice seed germination and seedling growth under Hg stress. (A) Photographic images (top) show representative seedlings at 3 and 7 days after sowing on MS medium containing 100 μM Hg, with or without 50 μM Cys or GSH. Graphs (bottom) show germination rates of seeds grown on MS medium supplemented with 50, 100, or 200 μM Hg, with or without 50 μM Cys or GSH, recorded over 6 days. (B) Photographic images (top) show representative seedlings 3 days after transferring germinated seeds to MS medium containing 50 or 100 μM Hg, with or without 50 μM Cys or GSH. Bar graph (bottom) presents the corresponding measurements of seedling growth. Data are presented as mean ± SD of three biological replicates. Different letters indicate significant differences (one-way ANOVA with Tukey's HSD test, $P < 0.05$).

Effects of Cys and GSH on Hg accumulation in rice

Rice plants were exposed to $HgCl_2$ at concentrations of 5 nM, 50 nM, and 20 μM for 24 h in a hydroponic system. Across all treatments, Hg predominantly accumulated in the roots compared to that in the shoots (Fig. 2B). Even with the application of Cys and GSH, Hg predominantly accumulated in the roots compared to that in the shoots. Cys application significantly increased Hg accumulation in the roots under all Hg stress conditions, whereas GSH application significantly reduced Hg accumulation in the roots compared to that of Hg stress alone. In contrast to roots, exogenous Cys and GSH exhibited no significant effect on Hg accumulation in the shoots. Hg contents in the root cell fractions—including the cell wall, cell organelles, and soluble fraction (cytoplasm)—were determined using rice roots treated with 20 μM, with or without Cys and GSH (Fig. 2B). Hg accumulation in the cell wall was much higher than that in the cytoplasm and cell organelles across all treatments. Exogenous Cys significantly increased Hg accumulation in the cell wall, whereas exogenous GSH significantly reduced it.

Effects of Cys and GSH on subcellular Hg distribution in rice root cells

To gain a more detailed understanding of the effects of Cys and GSH on intracellular Hg accumulation, distribution, and root cell organelle changes, TEM analysis was conducted (Fig. 2C). Hg accumulation within the cell organelles was observed as dark spots. Application of Cys, compared to that of Hg treatment alone, significantly increased Hg accumulation across all cell organelles, as indicated by the dark coloration. Hg was particularly abundant in the cell wall, intercellular spaces, and vacuoles. However, exogenous GSH significantly reduced Hg distribution within the cell organelles, although a higher Hg concentration was observed within the larger vacuoles than that in Hg treatment alone.

Changes in cell organelles were observed under Hg stress, with or without Cys and GSH. TEM analysis showed that control root cell organelles exhibited well-defined, thin cell walls and normal cell organelles, such as mitochondria, cell nucleus, and smaller vacuoles (Fig. 2C). Hg treatment partially destroyed the cell wall, while Cys and GSH maintained the cell wall integrity, and Cys significantly increased cell wall thickness. The number and size of vacuoles increased with the addition of Cys and GSH. Hg treatment significantly decreased the number of mitochondria and disrupted their structure. Conversely, the application of Cys and GSH maintained mitochondrial structure. Notably exogenous GSH increased the number of mitochondria.

FTIR spectra of Cys and GSH with Hg complexes

It is known that Hg has strong binding affinity with thiol (SH) groups of Cys and GSH in vitro (Kim et al., 2017, 2022). To identify molecular interaction between Hg^{2+} ions and functional groups of Cys or GSH molecules in root tissues, FTIR spectral analysis was performed (Fig. S1). A comparative analysis of the FTIR spectra for free Cys and GSH revealed distinct spectral changes indicative of complex formation by Hg ion. N–H stretching bands in 3200–3400 cm^{-1} showed slight shift or

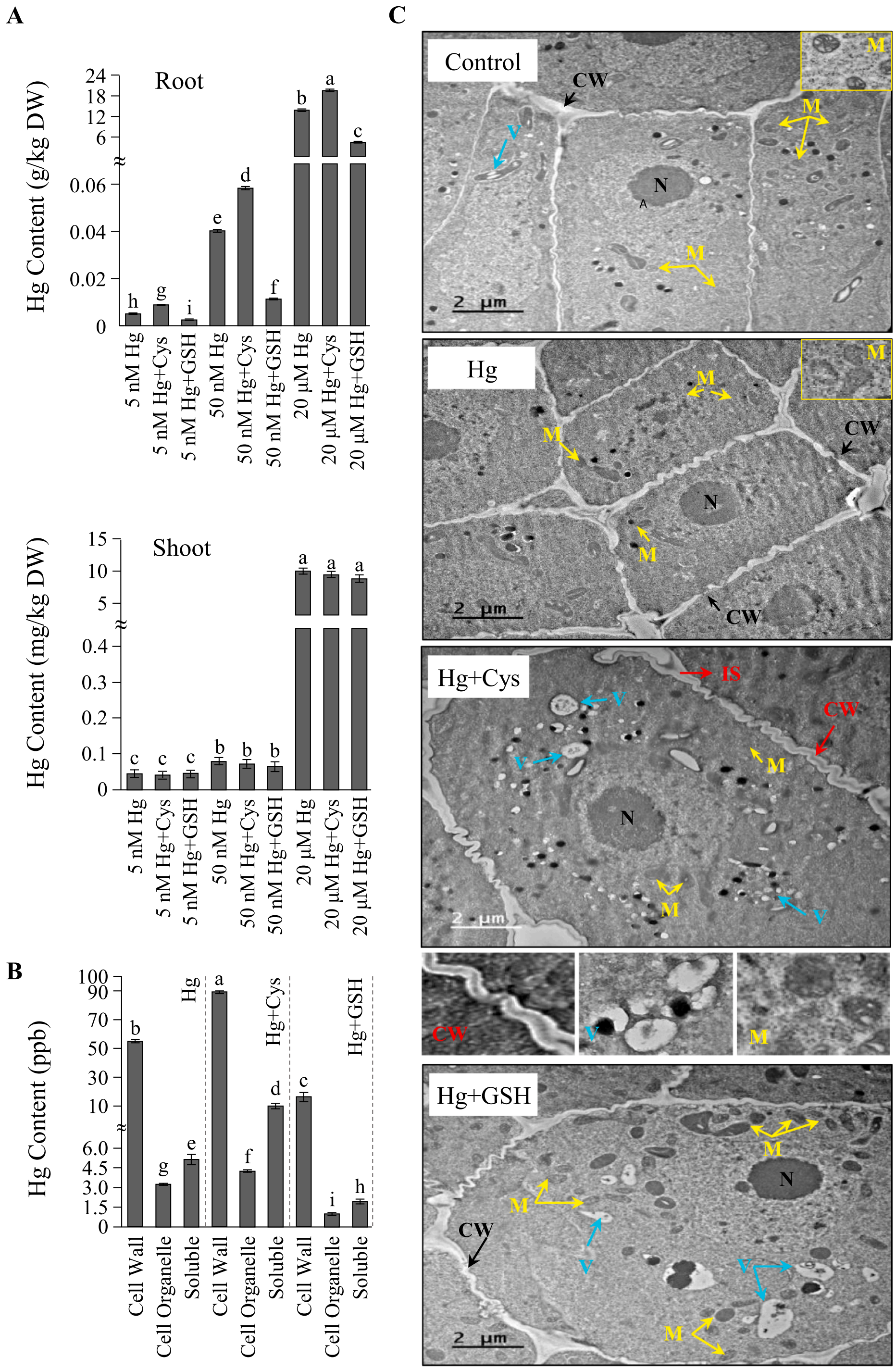

Fig. 2. Effects of exogenous Cys and GSH on Hg accumulation and subcellular distribution in rice roots. (A) Two-week-old rice were treated with 5 nM, 50 nM, and 20 μM Hg with 50 μM Cys or GSH for 24 h. Hg content in roots and shoots were quantified. Data are presented as mean ± SD of three biological replicates. Different letters indicate significant differences (one-way ANOVA with Tukey's HSD test, $P < 0.05$). (B) Rice roots were exposed to 20 μM Hg with or without 50 μM Cys or GSH for 24 h, and Hg contents in the fractions of cell wall, cell organelle, and soluble (cytoplasm) of rice roots were quantified. Data are presented as mean ± SD of three biological replicates. Different letters indicate significant differences (two-way ANOVA with Tukey's HSD test, $P < 0.05$) (C) Cellular Hg distribution and ultrastructural alterations observed by transmission electron microscopy (TEM). Rice roots were treated to 20 μM Hg with or without 50 μM Cys or GSH for 24 h. Scale bars = 2 μm. CW, cell wall; V, vacuole; M, mitochondria; IS: intercellular space.

intensity change in free Cys and broader peak in Hg+GSH in the presence of Hg, suggesting the possible change in hydrogen bonding or indirect effect due to structural changes. The S–H stretching region (~2550 cm^{-1}) in Hg+Cys showed an absent or diminished spectrum, and that in Hg+GSH showed absent the thiol (-SH) peak, which indicate Hg–S bond formation and strongly suggests binding of Hg^{2+} to the thiol group of Cys. COOH group (~1400–1700 cm^{-1}) in both Cys and GSH showed slight shift or change in intensity by Hg treatment, suggesting that Cys and GSH's carboxylic acid group might experience minor coordination after Hg binding. Hg+Cys shows sharper and more distinct peaks, particularly in COO^- and NH_2 regions due to its simpler structure compared to Hg+GSH.

Effects of Cys and GSH on cellular damage under Hg stress

Next, we investigated the effects of Cys and GSH on alleviating cellular damage, including destruction of cellular structures and cell membrane, and oxidative stress, in the presence of Hg in rice roots. PI staining, a marker of compromised membrane integrity and cell death (Truernit and Haseloff, 2008), revealed clear differences in root cell viability among treatments. In the control roots, PI fluorescence was minimal and uniformly faint, indicating largely intact and viable cells. In contrast, roots exposed to Hg exhibited markedly increased PI fluorescence, with distinct punctate and diffuse bright red signals throughout the tissue, signifying extensive loss of cell membrane integrity and widespread cell death (Fig. 3A). Exogenous Cys and GSH yielded PI staining patterns similar to those of control roots, indicating that they protected cellular structure and reduced membrane damage under Hg exposure. Further experiments clearly showed that Cys and GSH significantly alleviate lipid peroxidation and the loss in plasma membrane integrity. Significantly increased H_2O_2 by Hg stress was also reduced by exogenous Cys and GSH (Fig. 3B). Evaluation of cell viability using Evans blue staining showed that Hg stress markedly increased staining intensity, while Cys or GSH exhibited noticeably lower staining intensity. Spectrophotometric quantification confirmed these trends, demonstrating that both Cys and GSH significantly mitigated Hg-induced loss of cell viability (Fig. 3C). The staining with Schiff's reagent highlights the lipid peroxidation of the membranes through an intense red coloring (Yamamoto et al., 2001). Hg treatment increased the red signal in the roots compared to control (Fig. 3D). By contrast, the intensity of staining in the presence of Cys and GSH was relatively less than Hg treatment alone.

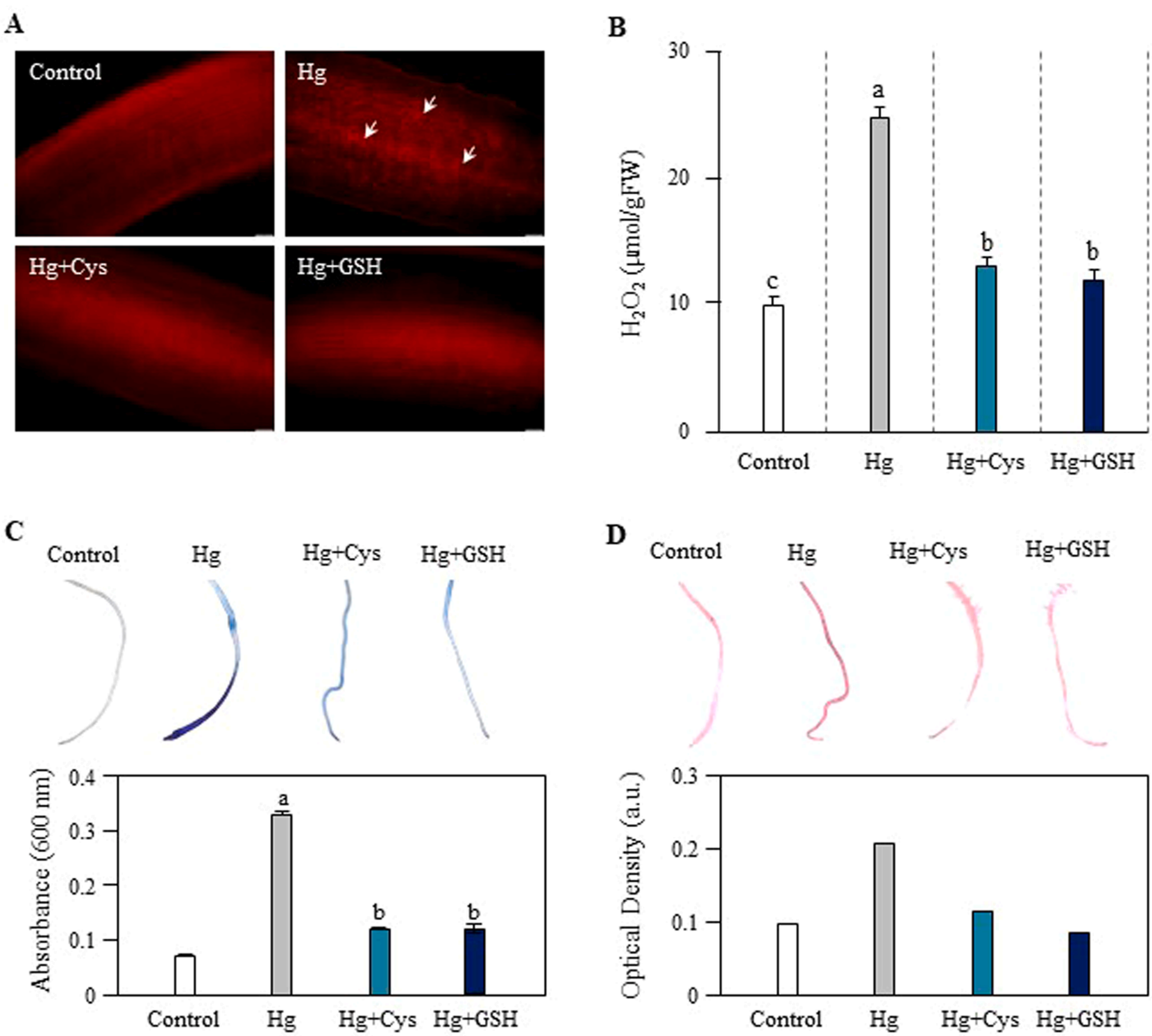

Fig. 3. Effects of exogenous Cys and GSH on cellular damage in rice roots. (A) Cell viability assessed after 24 h exposure to 20 µM Hg with or without 50 µM Cys or GSH using propidium iodide staining. Arrows indicate damaged cells. Scale bars = 100 µm. (B) H_2O_2 accumulation in rice roots after 24 h of treatment. (C) Cell membrane damage visualized by Evans blue staining. (D) Detection of lipid peroxidation using Schiff's reagent. Staining intensity was quantified using image J. Data in (B–D) are presented as mean ± SD of three biological replicates. Different letters indicate significant differences (one-way ANOVA with Tukey's HSD test, $P < 0.05$).

Identification and analysis of differentially expressed genes by RNA-Seq

To understand why Cys and GSH exhibit opposing effects on Hg accumulation in rice roots despite contributing equally to Hg tolerance, we investigated the molecular mechanisms underlying Hg uptake, transport, and detoxification mediated by exogenous Cys and GSH. A comparative transcriptome analysis (RNA-Seq) was conducted using RNA extracted from rice roots treated with or without 20 μM Cys and GSH in the presence of 20 μM $HgCl_2$ for 24 h. In this study, putative DEGs in rice roots were identified based on the following criteria: a log2 FC ≥ 1 for upregulated and ≤ 1 for downregulated DEGs, with a corrected P value < 0.01. RNA-Seq analysis and the corresponding MA plot showed 3152 (2203 upregulated and 949 downregulated genes), 1704 (1440 upregulated and 264 downregulated genes), and 295 DEGs (159 upregulated and 136 downregulated genes) in the Hg, Hg+Cys, and Hg+GSH treatments, respectively (Fig. 4A-B). Venn diagram analysis revealed that only 7 and 15 genes were commonly upregulated and downregulated, respectively, across all Hg, Hg+Cys, and Hg+GSH treatments (Fig. 4C). Hg and Hg+Cys treatments commonly upregulated and downregulated 1220 and 190 genes, respectively. In Hg and Hg+GSH comparison, 10 upregulated and 22 downregulated genes were commonly observed. While 980, 218, and 147 DEGs were upregulated by Hg, Hg+Cys, and Hg+GSH, respectively, 752, 59, and 99 DEGs were specifically downregulated in each treatment (Fig. 4C). These findings indicate that Hg treatment predominantly affects genes that are more responsive to Hg+Cys than to those of Hg+GSH. Hg+Cys and Hg+GSH upregulated 92 (27.2 %) of 338 DEGs and 1462 (85.6 %) of 1708 DEGs, respectively, compared to those of Hg treatment, whereas they downregulated 86 (17.1 %) of 502 DEGs and 2507 (85.8 %) of 2923, respectively (Fig. S2A-C). As shown in the Venn diagrams, 246 upregulated and 416 downregulated DEGs were commonly identified between the Hg+Cys and Hg+GSH treatments—substantially much more than those shared with the control group (Fig. S2C). The complex transcriptional patterns of DEGs were visualized by hierarchical clustering heat map analysis. Upregulation and downregulation of the C1 and C2 clusters were observed under Hg and Hg+Cys treatments, while Hg+GSH showed no significant changes in these clusters (Fig. 4D-E). Hg+GSH downregulated C1 and C2 gene clusters compared to those of Hg treatment, while Hg+Cys and Hg+GSH upregulated genes within the C3 cluster (Fig. S2D-E).

Gene ontology enrichment of differentially expressed genes

To identify the possible functional roles of DEGs responding to Hg, Hg+Cys, and Hg+GSH, Gene Ontology (GO) enrichment analysis was conducted. The DEGs were categorized into three major GO domains, including molecular function (MF), biological process (BP), and cellular component (CC) (Fig. 5). Most upregulated DEGs by Hg and Hg+Cys were more highly enriched in MF than in BP and CC. The Hg-induced DEGs categorized under MF primarily induced genes involved in binding (e.g., DNA, heme, vitamin B6, cation, and metal ion) and catalytic activities (e.g., transferase, oxidoreductase, and acyltransferase). Additionally, a relatively small number of DEGs were enriched in the BP category—primarily related to primary metabolic processes and protein modification—and in the CC category, including the apoplast, extracellular region, and ubiquitin ligase complex (Fig. 5A). Similar to Hg treatment, exogenous Cys highly enriched genes are involved in MF and BP categories. These findings indicate that the 1220 DEGs commonly upregulated by Hg and Hg+Cys treatments are highly enriched in BP and MF, as described above (Fig. 5B). In contrast to Hg and Hg+Cys treatments, Hg+GSH upregulated a smaller subset of DEGs, primarily associated with BP terms such as transmembrane transport and establishment of localization, CC terms related to membrane, and MF terms including transporter, small molecule sensor, phosphorelay sensor kinase, phosphotransferase, and protein histidine kinase activities (Fig. 5C). Kyoto Encyclopedia of Genes and Genomes (KEGG) pathway analysis (Fig. S3) showed patterns of upregulated DEGs consistent with those identified in the GO analysis for each treatment condition. Hg and Hg+Cys treatments led to significantly more upregulated genes than those of Hg+GSH, such as those involved in folding, sorting and degradation, environmental adaptation, signal transduction, metabolism of amino acids, carbohydrate, and lipid, as well as the biosynthesis of secondary metabolites. On the other hand, the 190 DEGs commonly downregulated by Hg and Hg+Cys were highly enriched in phosphorylation, stress response, and protein kinase activity (Fig. S4). Conversely, Hg+GSH downregulated DEGs associated with primary metabolic processes, ion and nucleic acid binding, and catalytic activities, showing no overlap in GO terms with Hg treatment (Fig. S4).

Exogenous GSH modulated significantly more genes—upregulated or downregulated—than those of exogenous Cys compared to Hg stress (Fig. S5). The 92 most highly enriched upregulated DEGs by Cys were primarily involved in catalytic activities and ion binding, while the downregulated DEGs were associated with carbohydrate metabolism and small molecule processes. Conversely, exogenous GSH additionally upregulated a number of DEGs, including those related to BP, binding, and catalytic activity, while downregulated BP genes were primarily involved in phosphorus metabolism, protein modification, binding, and catalytic activities.

Expression of cell wall synthesis-related genes and lignin accumulation

Polysaccharides—including components of plant cell walls such as cellulose, hemicellulose, lignin, and pectin—play a crucial role in binding HMs and preventing their entry into the plant cytoplasm (Cheng et al., 2025; Jia et al., 2019; Liang et al., 2022; Voiniciuc et al., 2018). Given that Hg is primarily retained in the root cell wall (Fig. 2), we investigated the transcriptomic changes in genes involved in cell wall biosynthesis, focusing on lignin, cellulose, and pectin, and validated the differential expression results from RNA-Seq using qRT-PCR analysis (Fig. 6, Table S2). Cellulose synthase genes— *OsCslF1, OsCslF2*, and *OsCslF3*—were upregulated by Hg and Hg+Cys, and their levels in Hg+Cys were higher than those in Hg treatment. In Hg+Cys, *OsCslF1* and *OsCslF2* exhibited higher expression levels than Hg+GSH, but *OsCslF3* showed similar level with Hg+GSH, according to RNA-Seq data and qRT-PCR analysis. Pectin biosynthesis enzymes, including galacturonyltransferase *OsGATL2*, *OsGATL4*, and *OsGATL6*, were induced 4–7 fold by Hg and Hg+Cys, but not by Hg+GSH. Genes involved in lignin biosynthesis tend to be induced by Hg and Hg+Cys but not by Hg+GSH (Table S2). In RNA-Seq results, the most significantly upregulated lignin synthesis genes, *OsC4H* and *OsC4H1*, were highly induced by Hg (16–18 fold) and Hg+Cys (25–28 fold). Additionally, *Os4CL5,* and *OsCCR13* showed approximately 10-fold induction under Hg and Hg+Cys treatments. qRT-PCR confirmed the same expression pattern (Fig. 6C). The expression levels of all these genes were higher in Hg+Cys. Other lignin synthesis genes, including *OsPAL04, OsPAL05, OsC4H2, OsCCR17,* and *OsCAD8D*, exhibited varying levels of induction (> 3-fold) in response to Hg and Hg+Cys. Lignin quantification using acetyl bromide showed that Hg significantly increased lignin content compared with control. Hg+Cys showed pronounced increase relative to Hg alone. Conversely, lignin content in the Hg+GSH was reduced compared with Hg treatment and remained close to control. Microscopic observation revealed clear treatment-dependent differences in lignin deposition (Fig. 6D-E). Very low lignin accumulation in control and Hg+GSH was detected, whereas Hg noticeably enhanced lignification, particularly in the cortex (CO). Hg+Cys further intensified lignin deposition in the exodermis (EX), and epidermis (EP), and central stele (ST), indicating widespread induction of secondary cell wall formation. These results indicate that Cys strongly promotes Hg-induced lignification in rice roots, whereas GSH suppresses this response.

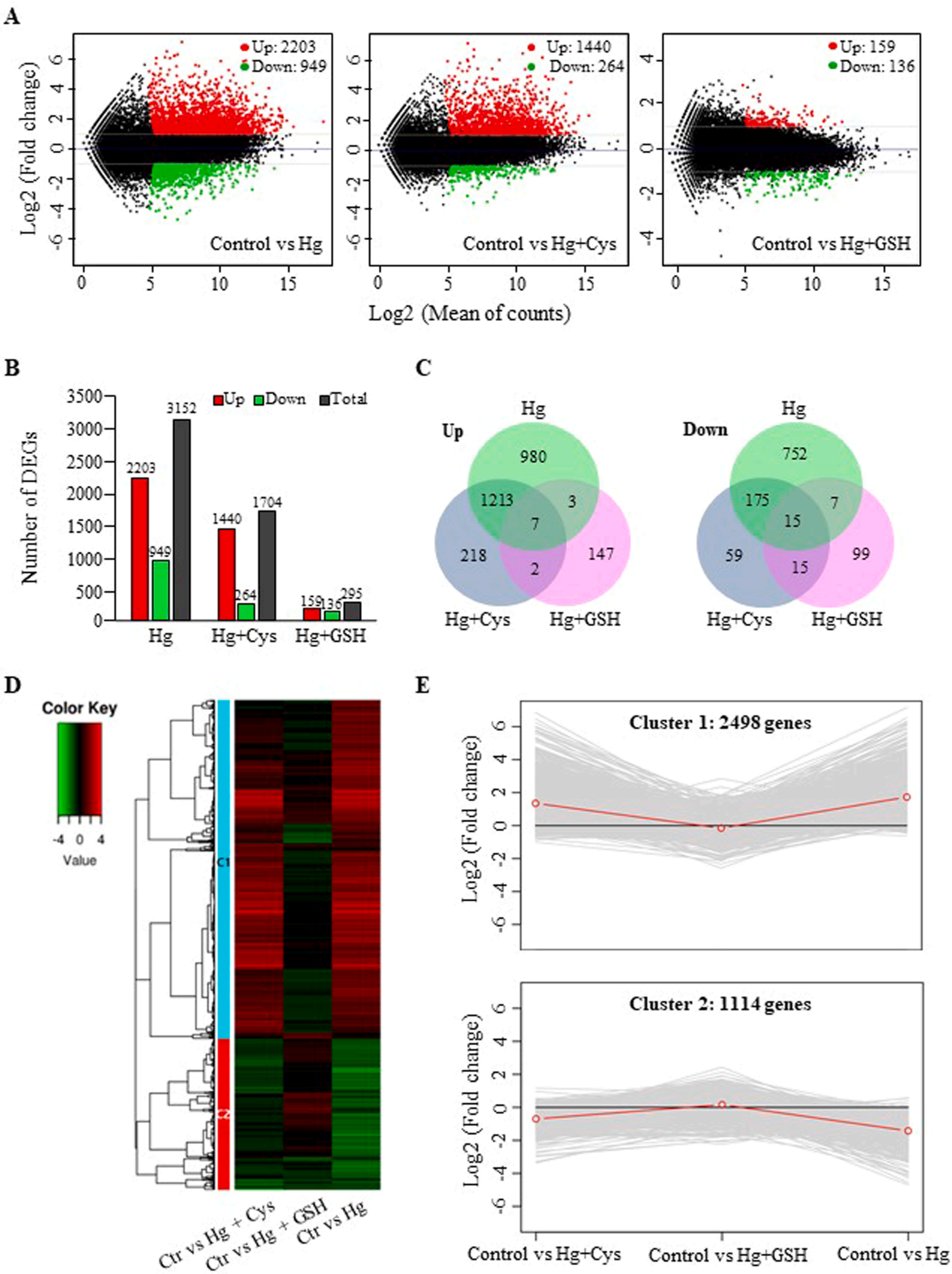

Fig. 4. RNA-Seq profiling of rice roots under Hg treatment with or without Cys or GSH. (A) MA plot representation of differentially expressed genes (DEGs). Red and green dots indicate significantly up- or downregulated genes (FDR < 0.01). (B) Numbers of upregulated and downregulated DEGs. (C) Venn diagram showing the number of common and specific DEGs in Hg, Hg+Cys, or Hg+GSH. (D) Heatmap of hierarchical clustering. Red indicates up-regulation and green indicates down-regulation. (E) Line plot for clustering DEG. The red line represents the overall expression tendency in each cluster.

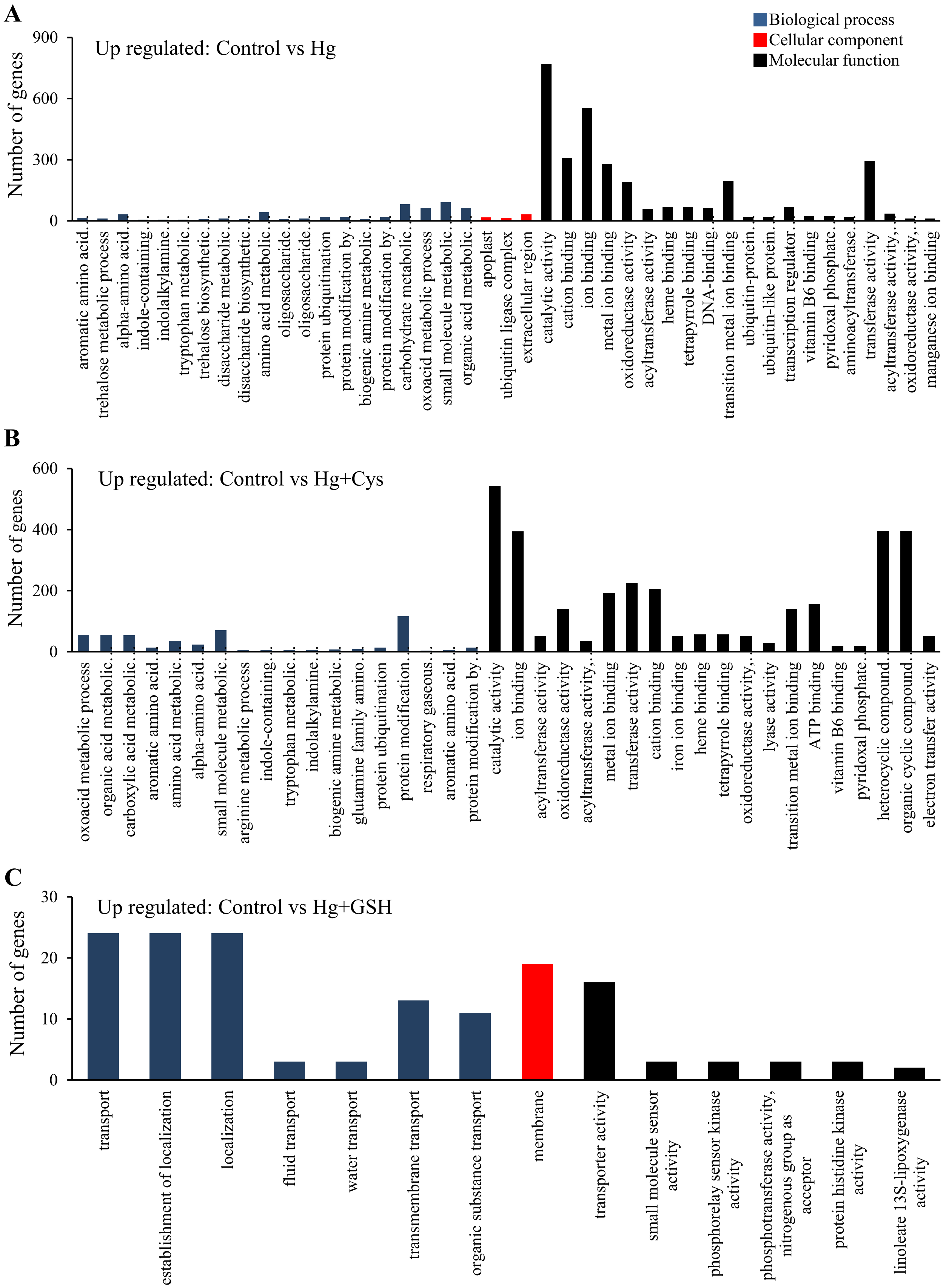

Fig. 5. Gene Ontology (GO) enrichment analysis of upregulated DEGs. GO terms enriched in biological processes (green), molecular functions (red), and cellular components (black) are shown for upregulated DEGs relative to the control.

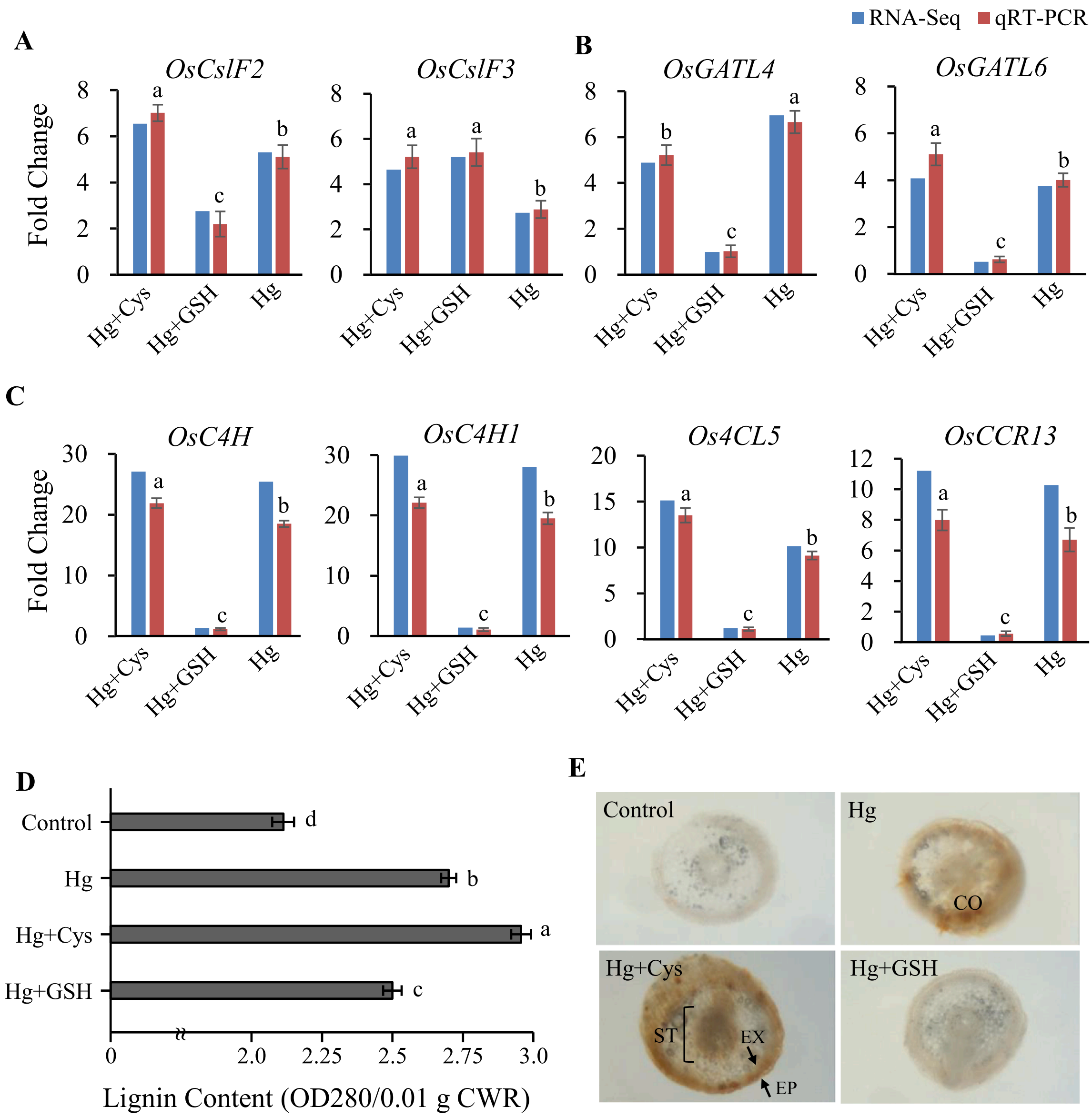

Fig. 6. Validation of cell wall synthesis genes and lignin accumulation. (A–C) qRT-PCR validation of RNA-Seq-identified genes involved in cellulose (A), pectin (B), and lignin (C) biosynthesis. (D) Lignin content in rice roots was determined by acetyl bromide. Data are presented as mean ± SD of three biological replicates. Different letters indicate significant differences among treatments (one-way ANOVA with Tukey's HSD test, $P < 0.05$). (E) Histochemical detection of lignin in rice roots. CO, cortex; ST, stele; EX, exodermis; EP, epidermis.

Expression of membrane transporter genes

Given that understanding how Cys and GSH differentially modulate Hg accumulation and contribute to Hg tolerance is essential, we investigated candidate genes involved in Hg transport and detoxification (Table S2). RNA-Seq and KEGG pathway analyses revealed a significant upregulation of ATP-binding cassette (ABC) transporter genes in response to Hg and Hg+Cys treatments. Therefore, in this study, we investigated the regulation patterns of ABC transporters.

Hg and Hg+Cys treatments upregulated numerous ABC transporter genes, exhibiting significantly higher expression levels than those observed under Hg+GSH. In plants, ABC transporters are categorized into eight subfamilies, such as ABCA-ABCG and ABCI (Kang et al., 2011). Among these, genes belonging to the G subfamily were most prominently induced by Hg and Hg+Cys, whereas Hg+GSH exhibited minimal effect (Table S2). Among the genes, several OsABCGs members—such as *OsABCG3, OsABCG9, OsABCG27, OsABCG35, OsABCG39, OsABCG41, OsABCG44, OsABCG45,* and *OsABCG48*—exhibited higher expression levels in Hg+Cys than those in Hg. The qRT-PCR result showed similar expression patterns for *OsABCG3, OsABCG9, OsABCG27, OsABCG39, OsABCG45,* and *OsABCG48* (Fig. 7). Relatively small numbers of other subfamilies—including *OsABCA4*, *OsABCB6*, *OsABCB9*, *OsABCB10*, *OsABCB11*, and *OsABCC3* —were significantly upregulated by Hg and Hg+Cys treatments (approximately 3- to 13-fold) but not by Hg+GSH, and the expression patterns of *OsABCB6*, *OsABCB11*, and *OsABCC3* were reconfirmed by qRT-PCR (Fig. 7). Conversely, Hg+GSH-specific induced genes such as *OsABCB27*, *OsABCG14*, and *OsABCG49* were observed. The significant induction of multiple ABC transporters suggests possible involvement in Hg handling during Cys-mediated Hg response.

Excess metal ions decrease water absorption by roots, leading to water deficit (Rucińska-Sobkowiak, 2016). Aquaporins (AQPs) are transmembrane channels that facilitate the passive transport of water and other small molecules across cellular membranes (Przedpelska-Wasowicz and Wierzbicka, 2011; Shivaraj et al., 2019).

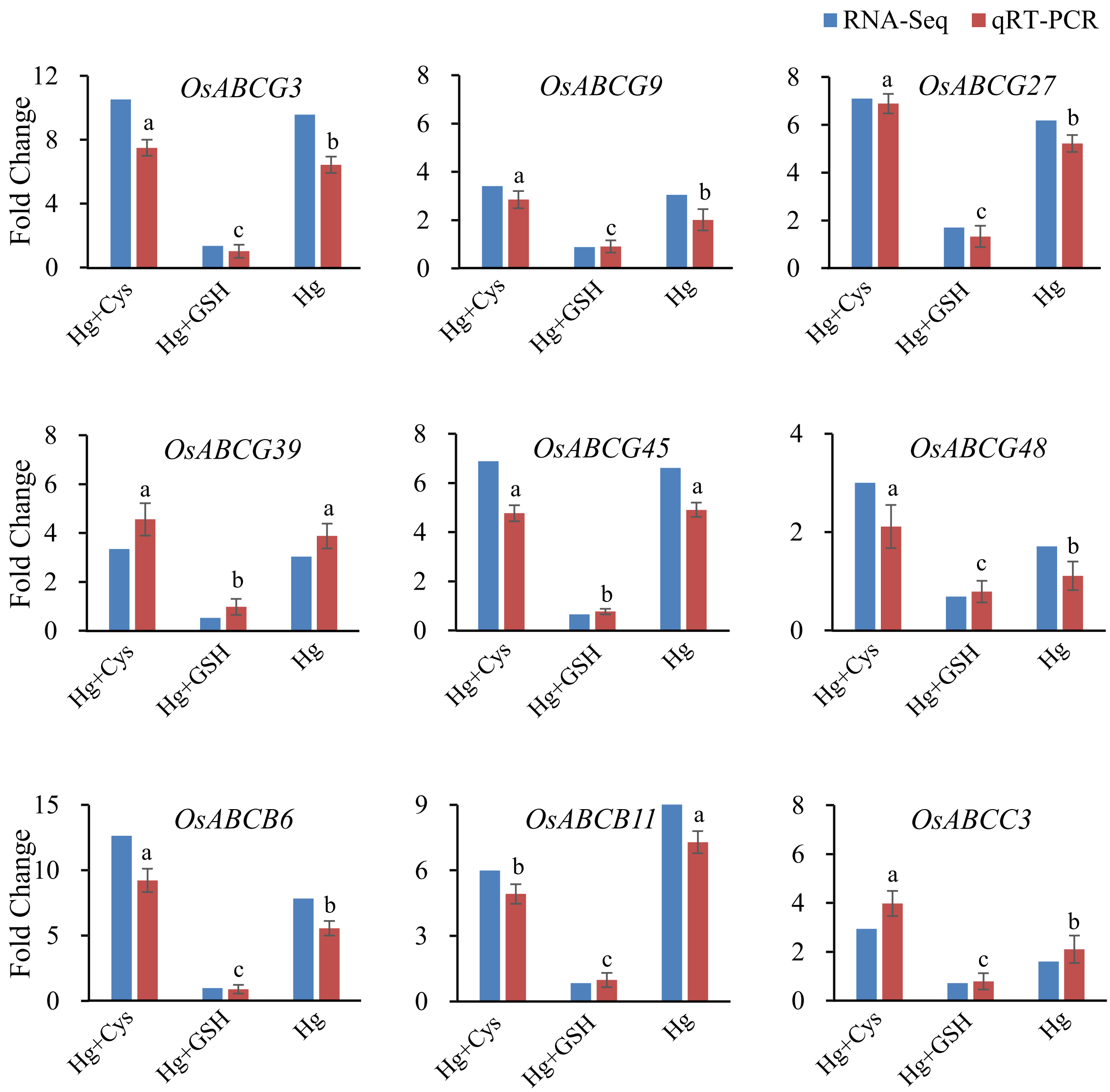

Fig. 7. Validation of ABC transporter genes by qRT-PCR. Expression of selected target genes from the RNA-Seq analysis were validated by qRT-PCR. Data are presented as mean ± SD of three biological replicates. Different letters indicate significant differences (one-way ANOVA followed by Tukey's HSD test, $P < 0.05$).

They are considered key candidates involved in HM tolerance. Hg and Hg+Cys treatments downregulated several AQP genes, such as PIPs, NIPs, and TIPs, with Hg showing lower expression levels than that in Hg+Cys (Table S2). However, Hg+GSH treatment upregulated a significant number of AQP genes, including PIP (*OsPIP1–2, OsPIP2–1, OsPIP2–2, OsPIP2–3, OsPIP2–6,* and *OsPIP2–7*), OsTIP (*OsTIP1–1, OsTIP1–2*, and *OsTIP2–2*), and OsNIP genes (*OsNIP1–2, OsNIP2–1, OsNIP2–2*, and *OsNIP3–1*).

Expression of antioxidative enzyme genes

Upon entry into plant cells, free Hg ions generate excessive ROS, leading to significant damage to cellular organelles. Since ROS scavenging plays an important role in enhancing Hg tolerance, we investigated the transcriptomic changes in antioxidant enzyme genes in response to exogenous Cys and GSH (Table S2). Hg and Hg+Cys upregulated *OsGR2* and *OsGR3* at similar levels, and Hg+Cys upregulated *OsCATC* but was not observed under Hg stress. Hg and Hg+Cys significantly upregulated several peroxidase genes (*OsPOD2, Osprx22, Osprx62, Osprx70, Osprx81, Osprx82, Osprx83, Osprx84, Osprx85,* and *Osprx86*), with Hg+Cys showing lower expression levels than those in Hg. Notably, *Osprx84* and *Osprx85* were highly induced, with 15- and 37-fold increases by Hg, respectively. In contrast to Hg and Hg+Cys, Hg+GSH did not significantly induce peroxidase but induced SOD (*OsFeSOD1*) and catalase (*OsCATA*).

Discussion

Cys and GSH enhance Hg tolerance but differentially regulate Hg accumulation and cellular distribution

Mercury is readily absorbed by plant roots, highlighting the need to understand the underlying mechanisms governing Hg transport, accumulation, and tolerance in crop species. Previous studies show that exogenous Cys and GSH significantly enhance Hg tolerance in *Arabidopsis thaliana*, though they regulate Hg accumulation differently (Kim et al., 2017, 2022). However, the mechanism by which Cys and GSH mediate Hg transport and cellular accumulation in plant roots remains unclear. Consistent with previous *Arabidopsis* findings, exogenous Cys and GSH exhibited positive effects on Hg tolerance during germination and seedling growth in rice (Fig. 1). These findings suggest that Cys and GSH play an important role in enhancing Hg tolerance in both dicotyledons and monocotyledons.

Notably, absorbed Hg was primarily retained in rice roots, with or without Cys and GSH. However, Cys and GSH applications significantly increased or reduced Hg accumulation in rice roots, respectively (Fig. 2A). These results strongly suggest that Cys and GSH have different regulatory mechanisms for Hg uptake and transport in root cells, as they do not significantly affect Hg transport from root to shoot. Cys application led to prominent Hg accumulation in the cell walls and intercellular spaces of rice roots (Fig. 2B-C). Since positively charged Hg ions can be strongly bound to the negatively charged root cell walls (Amos and Mohnen, 2019; Cheng et al., 2025), exogenous Cys may enhance the Hg binding capacity to the cell wall, thereby potentially reducing Hg influx into cells and its translocation from roots to shoots (Fig. 2B). In plant cells, vacuoles play a crucial role in the detoxification of HMs by sequestering them, preventing cellular damage and maintaining homeostasis. Therefore, Hg sequestration in the cell wall and vacuole observed in this study is thought to play an important role in protecting cells from Hg toxicity in roots (Fig. 3). Mitochondria are important organelles serving as the primary source of ATP through respiration. Mitochondrial dysfunction is a common phenomenon in HM-induced cytotoxicity (Keunen et al., 2011). The results of this study showed that Hg caused structural damage and reduced their numbers, but the mitochondrial structure was protected from Hg-induced damage by exogenous Cys and GSH (Fig. 2C). The changes of SH peak in both Cys and GSH spectrum by Hg treatment confirm that Hg binds preferentially to SH group of Cys and GSH in rice roots (Fig. S1). Both Cys and GSH showed additional changes in the C═O stretching and NH stretching by Hg, suggesting slight backbone involvement or structural changes. Collectively, these data clearly indicate the formation of a stable Cys– or GSH–Hg complex, resulting in reducing the possibility of Hg ions binding to mitochondrial nucleic acids. The significant increase in mitochondrial numbers with exogenous GSH suggests that GSH-mediated Hg tolerance is largely dependent on mitochondrial metabolic processes. Further biochemical or genetic evidence will be required to establish a mechanistic role for mitochondria in GSH-mediated Hg tolerance.

Transcriptomic divergence reveals distinct molecular responses to Cys and GSH under Hg stress

Although both Cys and GSH enhance Hg tolerance, understanding how they differently regulate cellular response pathway, including Hg transport, accumulation, and detoxification and remains of interest. RNA-Seq analysis revealed that Hg and Hg+Cys modulated and shared significantly more genes than those of Hg+GSH. Notably, the significantly increased metal ion binding genes is correlated with the strong Hg retention in cell organelles under Hg and Hg+Cys treatments. GO and KEGG enrichment analyses reveal that Hg and Hg+Cys highly enriched biological pathways related to protein modification, particularly protein ubiquitination pathways (Figs. 4–5, Fig. S3). This suggests that Cys increases the turnover of Hg-induced damaged or misfolded proteins, thereby activating proteotoxicity and metabolic stress responses. Similarly, enrichment of trehalose metabolic process points to activation of metabolic buffering mechanisms that stabilize proteins and membranes under Hg stress. These pathways, together with the induction of oxidoreductases, transferases, and signal-transduction genes, imply that Cys reinforces Hg-induced stress at both the protein and metabolic levels while also promoting Hg immobilization at the cell wall and limited internal transport. In contrast, GSH induced a much narrower transcriptional response mainly related to membrane transport and phosphorelay signaling (Fig. 5C, Fig. S5), suggesting that GSH-mediated Hg tolerance may be attributed to membrane maintenance and metabolic activation under Hg stress. The absence of strong enrichment for ubiquitination, trehalose metabolism, and other stress-related pathways under Hg+GSH suggests that GSH's efficient inhibition of Hg uptake reduces cellular stress and, consequently, minimizes the need for extensive proteostasis and metabolic adjustment.

Cys strongly induces genes involved in cell wall biosynthesis and lignification

As the first line of defense against HMs, plants employ strategies that restrict metal uptake and long-distance transport, largely by immobilizing metals within the cell wall (Hasan et al., 2015; Manara, 2012). HM exposure commonly induces the accumulation of major cell-wall polysaccharides—including cellulose, pectin, and lignin—thereby thickening the wall and promoting metal fixation (Krzesłowska et al., 2016; Liang et al., 2022; Liu et al., 2014; Voiniciuc et al., 2018). In our study, exogenous Cys significantly enhanced Hg sequestration in root cell walls (Fig. 2), making the molecular regulation of cell wall biosynthesis genes particularly relevant. Cellulose and pectin contain abundant carboxyl groups capable of binding metal ions (Cheng et al., 2025; Li et al., 2022). Recent work further demonstrates that exogenous Cys can reduce Cd translocation Chinese cabbage by enhancing Cd retention in the root cell wall pectin (Li et al., 2024), highlighting amino acids as important modulators of apoplastic detoxification pathways. In our study, Hg-induced genes associated with cellulose (*OsCslF1*, *OsCslF2*, *OsCslF3*) and pectin biosynthesis (*OsGATL2*, *OsGATL4*, *OsGATL6*) were similarly or even more strongly upregulated by Cys application (Fig. 6; Table S2), supporting a broader role of amino acids in fortifying the apoplastic barrier and restricting HM mobility through coordinated stimulation of cell wall polysaccharide synthesis. Lignin biosynthesis also plays a crucial role in HM tolerance. We observed significant induction of key lignin-associated genes in Hg-treated roots, with several (*OsC4H*, *OsC4H1*, *Os4CL5*, *OsCCR13*) further upregulated by Cys. These expression patterns closely matched the observed lignin accumulation in rice roots (Fig. 6D-E). While GSH did not increase lignin accumulation relative to the control, Hg alone elevated lignin in both the cortex and central stele, and Cys treatment led to even stronger lignification in the stele and outer tissues such as the epidermis. Lignin accumulation is a common adaptive response to various metals, including Cd (Dong et al., 2023), Cu (Chen et al., 2002; Zhou et al., 2025), and Al (Mao et al., 2004), and reduced lignin content has been linked to heightened Hg sensitivity in maize (Shao et al., 2022). The abundant functional groups in lignin such as hydroxyl, methoxyl, and carboxyl groups likely facilitate efficient Hg binding at the root surface (Cheng et al., 2025; Zhang et al., 2023), while lignification of the stele restricts Hg entry into the vascular system and thereby limits systemic translocation. On the other hand, lignin assembly requires transport of monolignols and related precursors. Plant ABCG transporters mediate the efflux of such metabolites, and their upregulation under HM stress suggests coordination with lignin biosynthetic pathways (Takeuchi et al., 2018). Thus, the Cys-induced activation of lignin biosynthesis may be complemented by enhanced ABCG transporters (Table S2), which mediate the transport of lignin precursors, thereby promoting efficient polymerization and reinforced cell wall deposition. Beyond the plant cell wall, the effectiveness of Cys and GSH in phytoremediation should be considered within the ecological context of the rhizosphere microbiome. Microbiome influence Hg speciation, mobility, and plant stress responses (Lang et al., 2025), suggesting that integrating Cys/GSH treatments with microbiome-aware soil management could improve Hg immobilization.

Cys and GSH differently regulate membrane transporters

The next question is how Hg can enter across cell membranes, since Cys application increases Hg import into the cells. Heavy metal ions, due to their charge, require active transport systems which requires energy and specific transporters to cross cell membranes. HMs are transported across cell membranes through diffusion and active transport which requires energy and specific transporters. Hg may be absorbed and transported via transporters or channels of other HM and nutrient. To gain insight into Hg transport, we examined the expression of several transporter families—such as NRAMPs, ZIPs, MTP, CAXs, CCXs, VTLs, OPTs, ECAs, and ABC—associated with plasma and tonoplast membrane. Among these, ABC transporters showed the clearest transcriptional response to Hg exposure based on our GO and KEGG enrichment analyses. Notably, Hg strongly induced larger number of G-type ABC transporters, and several OsABCG genes (3, 9, 27, 35, 37, 39, 41, 44, 45, and 48) were further upregulated under Hg+Cys treatment (Fig. 7, Table S2). Studies show that *OsABCGs* (*9, 31, 36,* and *43*) which are induced by Cd, As, and Zn, play direct roles in the transport and accumulation of these metals (Chen et al., 2011; Fu et al., 2019; Moons, 2003, 2008; Oda et al., 2011; Tian et al., 2023; Yu et al., 2012). Given the strong induction of several OsABCG transporters under Hg treatment, they likely play a preferential role in handling Hg-derived substrates. Because Cys readily binds Hg to form stable Hg–Cys complexes (Fig. S1), rice roots are likely to encounter Hg predominantly in this chelated form under Cys-enriched conditions. In this context, the strong induction of OsABCG genes and increased intracellular Hg content in the presence of Cys suggests the import of Hg–Cys complexes, supporting the hypothesis that these transporters act as Hg importers. To determine whether these OsABCGs mediate influx, efflux, or sequestration of Hg or Hg–Cys complexes, localization, heterologous transport assays, and mutant analysis will require. *OsABCB6* and *OsABCB9* are upregulated by salt stress, while *OsABCB11* is induced by drought (Saha et al., 2015; Zou et al., 2025). In this study, these genes were induced by Hg and Hg+Cys (Table S2), indicating their potential involvement in both Hg transport and broader abiotic stress responses. Moreover, vacuolar compartmentalization is a general adaptive strategy that plants use to cope with HM stress. *AtABCC1, AtABCC2,* and *AtABCC3* are known as important vacuolar transporters that contribute to tolerance against Cd and Hg (Brunetti et al., 2015; Park et al., 2012). In this study, the additional upregulation of ABCC transporters (*OsABCC2, 3,* and *15*) by exogenous Cys suggests their potential role in transporting Hg from the cytosol to the vacuole (Fig. 8), thereby reducing intracellular Hg toxicity. A more detailed analysis of subcellular localization of the induced genes is necessary to clarify the relationship between ABC transporter gene expression and Hg transport.

Heavy metal exposure can affect water uptake and transport by reducing the water permeability of the cell membrane. AQPs—a family of integral membrane proteins—are believed to play a crucial role in HM stress tolerance by maintaining water balance under HM stress (Przedpelska-Wasowicz and Wierzbicka, 2011; Shivaraj et al., 2019). Our results showed that Hg significantly downregulated three types of AQPs (PIP, NIP, and TIP) (Table S2), which could interfere with water uptake and induce Hg sensitivity in rice roots. It has been suggested that plants compensate for HM-induced water stress by altering AQP expression or activity (Vats et al., 2021). Notably, Hg+GSH upregulated several AQP genes, including *PIPs* (*OsPIP1–2, 2–1, 2–2, 2–3, 2–6,* and *2–7*), *TIPs* (*OsTIP1–1, 1–2,* and *2–2*), and *NIPs* (*OsNIP1–2, OsNIP2–1, OsNIP2–2,* and *OsNIP3–1*), compared to those of Hg and Hg+Cys treatments. The increase in AQPs by Hg+GSH strongly reflects the GO enrichment results, which showed an increase in the expression of membrane-related genes in particular (Fig. 4C). GSH probably may alleviate Hg-induced water deficit by activating AQPs in the cell membranes, thereby contributing to Hg tolerance.

Differential activation of Cys- and GSH-mediated antioxidant pathways

Despite the large amount of Hg fixed in the cell wall, a significant

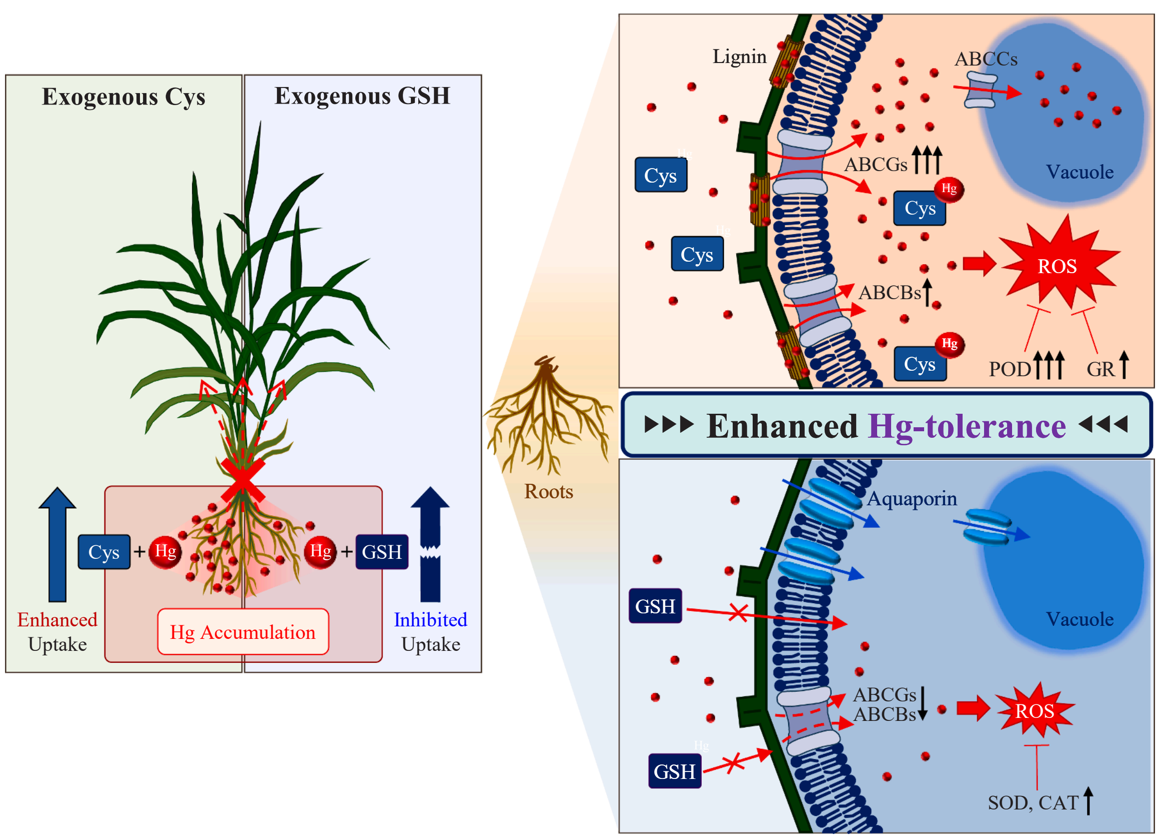

Fig. 8. Schematic diagram illustrating the proposed mechanisms by which exogenous Cys and GSH regulate Hg uptake, accumulation, and tolerance in rice roots. Exogenous Cys enhances Hg uptake and accumulation primarily by promoting Hg fixation to the cell wall via lignin biosynthesis and by upregulating ABC transporters, thereby facilitating intercellular Hg transport. In contrast, exogenous GSH suppresses Hg uptake and accumulation and enhances aquaporin expression. Both Cys and GSH alleviate Hg-induced oxidative stress; Cys enhances POD-mediated ROS scavenging, whereas GSH reduces ROS production by limiting intracellular Hg levels.

portion still enters the root cell membrane, leading to excessive ROS production in the cells and cellular damage (Fig. 3). Therefore, ROS scavenging is considered a crucial mechanism of Hg tolerance (Kim et al., 2017; Natasha et al., 2020). Exogenous Cys and GSH efficiently reduced Hg-generated ROS (e.g., H_2O_2) and alleviated oxidative damage in rice roots (Fig. 3). Previous study shows that Hg+Cys slightly induced *MnSOD1* and *GR1* in *Arabidopsis* roots (Kim et al., 2022), but primarily induced several *PODs* in rice roots (Table S2). This suggests that Cys preferentially stimulates the H_2O_2 scavenging pathway rather than that of the O_2^- scavenging pathway, clearly demonstrating that Cys actively reduces H_2O_2 levels through PODs, in addition to its role in directly scavenging ROS. Although *PODs* are also significantly induced by Hg, Hg generates ROS levels much higher than that of the scavenging capacity of the antioxidant system, which may result in oxidative stress and disruption of mitochondrial and cellular metabolism. In contrast, Hg+GSH treatment slightly induced *OsFeSOD1* and *CATA*. It is clear that GSH treatment reduced ROS production by keeping the intracellular Hg concentration very low (Fig. 2, Fig. 8). Therefore, although the expression of related genes is not as diverse as that of Cys, it may be sufficient to scavenge ROS and reduce oxidative damage.

Conclusion

This study demonstrated that exogenous Cys and GSH enhanced Hg tolerance in rice through distinct mechanisms. Cys promoted Hg accumulation in roots primarily by enhancing sequestration in the cell wall and intercellular spaces, likely through the lignin biosynthesis. This leads to physical immobilization of Hg and limits its cellular entry and long-distance transport. In contrast, GSH reduced Hg accumulation in roots and increased mitochondrial number with preserved mitochondrial structure. Transcriptome analysis revealed that Cys and Hg treatments showed commonly upregulated DEGs related to ion binding and cell wall metabolism. In contrast, GSH uniquely upregulated catalytic function and membrane-related genes including AQPs, suggesting roles in maintaining membrane function and water balance under Hg stress. Additionally, the strong induction of ABC transporter genes, especially *OsABCGs* and *OsABCCs*, by Hg and further by Cys indicates their potential roles in Hg transport into cells and vacuoles. Further studies are needed to elucidate specific roles of individual ABC transporters in Hg transport across the cell or vacuolar membranes based on the expression patterns of ABC transporter genes identified in this study. Both Cys and GSH effectively reduced Hg-induced ROS and oxidative damage, with Cys favoring the activation of POD-mediated H_2O_2 scavenging and GSH reducing ROS through minimizing intracellular Hg with slight induction of SOD and CAT. The data presented in this study offer new insights into the Cys- and GSH-mediated mechanisms of Hg tolerance and transport by investigating the gene responses associated with various metabolic pathways—including Hg cell wall binding, membrane transport, and ROS scavenging—in rice root cells during Hg stress (Fig. 8). Cys and GSH applications may be effective and feasible for removing Hg from contaminated soils using plants or for the cultivation of eco-friendly crop.

CRediT authorship contribution statement

Dream Kim: Visualization, Investigation, Data curation. **Yeon-Ok Kim:** Writing – original draft, Supervision, Project administration, Methodology, Investigation, Conceptualization. **Jangho Kim:** Writing – review & editing, Supervision, Project administration, Funding acquisition. **Mahpara Safdar:** Visualization, Investigation.

Funding

This work was supported by Korea Institute of Planning and Evaluation for Technology in Food, Agriculture and Forestry (IPET) through the Agriculture and Food Convergence Technologies Program for Research Manpower development, funded by Ministry of Agriculture, Food and Rural Affairs (MAFRA) (project no. RS-2024–00397026), and by a grant from the Basic Science Research Program through the National Research Foundation (NRF) of Korea, funded by the Ministry of Education (NRF-2018R1D1A1B07045677).

Declaration of Competing Interest

The authors declare that they have no known competing financial interests or personal relationships that could have appeared to influence the work reported in this paper.

Acknowledgments

We sincerely thank the Center for Research Facilities at the Chonnam National University for their assistance in the analysis of ICP, TEM, and FTIR

Appendix A. Supporting information

Supplementary data associated with this article can be found in the online version at doi:10.1016/j.envexpbot.2026.106312.

Data Availability

RNA-seq data used in this study have been deposited in the NCBI Gene Expression Omnibus database under accession number PRJNA625639.

References

Ajsuvakova, O.P., Tinkov, A.A., Aschner, M., Rocha, J.B.T., Michalke, B., Skalnaya, M.G., Skalny, A.V., Butnariu, M., Dadar, M., Sarac, I., Aaseth, J., Bjørklund, G., 2020. Sulfhydryl groups as targets of mercury toxicity. Coord. Chem. Rev. 417, 213343. https://doi.org/10.1016/j.ccr.2020.213343.

Amos, R.A., Mohnen, D., 2019. Critical review of plant cell wall matrix polysaccharide glycosyltransferase activities verified by heterologous protein expression. Front. Plant Sci. 10, 915. https://doi.org/10.3389/fpls.2019.00915.

Zou, H., Fan, C., Chen, X., Chen, R., Sun, Z., Wan, X., 2025. Genome-wide analyses of the soybean *GmABCB* gene family in response to salt stress. Genes 16, 233. https://doi.org/10.3390/genes16020233.

Aysin, F., Karaman, A., Yilmaz, A., Aksakal, Ö., Gezgincioglu, E., Kohnehshahri, S.M., 2020. Exogenous cysteine alleviates mercury stress by promoting antioxidant defence in maize (*Zea mays L.*) seedlings. Turk. J. Agric. For. 44, 506–516. https://doi.org/10.3906/tar-1909-2.

Azarakhsh, M.R., Asrar, Z., Mansouri, H., 2015. Effects of seed and vegetative stage cysteine treatments on oxidative stress response molecules and enzymes in *Ocimum basilicum* L. under cobalt stress. J. Soil Sci. Plant Nutr. 15, 651–662. https://doi.org/10.4067/S0718-95162015005000044.

Brunetti, P., Zanella, L., De Paolis, A., Di Litta, D., Cecchetti, V., Falasca, G., Barbieri, M., Altamura, M.M., Costantino, P., Cardarelli, M., 2015. Cadmium-inducible expression of the ABC-type transporter *AtABCC3* increases phytochelatin-mediated cadmium tolerance in *Arabidopsis*. J. Exp. Bot. 66, 3815–3829. https://doi.org/10.1093/jxb/erv185.

Chen, E.L., Chen, Y.A., Chen, L.M., Liu, Z.H., 2002. Effect of copper on peroxidase activity and lignin content in *Raphanus sativus*. Plant Physiol. Biochem. 40, 439–444. https://doi.org/10.1016/S0981-9428(02)01392-X.

Chen, G., Komatsuda, T., Ma, J.F., Nawrath, C., Pourkheirandish, M., Tagiri, A., Hu, Y.G., Sameri, M., Li, X., Zhao, X., Liu, Y., Li, C., Ma, X., Wang, A., Nair, S., Wang, N., Miyao, A., Sakuma, S., Yamaji, N., Zhenge, X., Nevo, E., 2011. An ATP-binding cassette subfamily G full transporter is essential for the retention of leaf water in both wild barley and rice. Proc. Natl. Acad. Sci. U. S. A. 108, 12354–12359. https://doi.org/10.1073/pnas.1108444108.

Chen, Y.A., Chi, W.C., Huang, T.L., Lin, C.Y., Quynh Nguyeh, T.T., Hsiung, Y.C., Chia, L.C., Huang, H.J., 2012. Mercury-induced biochemical and proteomic changes in rice roots. Plant Physiol. Biochem 55, 23–32. https://doi.org/10.1016/j.plaphy.2012.03.008.

Chen, Y.A., Chi, W.C., Trinh, N.N., Huang, L.Y., Chen, Y.C., Cheng, K.T., Huang, T.L., Lin, C.Y., Huang, H.J., 2014. Transcriptome profiling and physiological studies reveal a major role for aromatic amino acids in mercury stress tolerance in rice seedlings. PLoS One 9, e95163. https://doi.org/10.1371/journal.pone.0095163.

Cheng, Z., Wang, C., Tang, F., Zhou, Y., Zhu, C., Ding, Y., 2025. The cell wall functions in plant heavy metal response. Ecotoxicol. Environ. Saf. 299, 118326. https://doi.org/10.1016/j.ecoenv.2025.118326.

Dago, A., Ariño, C., Díaz-Cruz, J.M., Esteban, M., 2014. Analysis of phytochelatins and Hg-phytochelatin complexes in *Hordeum vulgare* plants stressed with Hg and Cd:

HPLC study with amperometric detection. Intern. Int. J. Environ. Anal. Chem. 94, 668–678. https://doi.org/10.1080/03067319.2013.864649.
Dong, Q., Tao, Q., Li, B., Huang, R., Xu, Q., Li, H., Shen, J., Chen, X., Li, Q., Tang, X., Kačík, F., Kováč, J., Ďurkovič, J., Wu, Y., Wang, C., 2023. The mechanism of enhanced lignin regulating foliar Cd absorption and yield in rice (*Oryza sativa* L.). Ecotoxicol. Environ. Saf. 249, 114481. https://doi.org/10.1016/j.ecoenv.2022.114481.
Ericksen, J.A., Gustin, M.S., 2004. Foliar exchange of mercury as a function of soil and air mercury concentrations. Sci. Total Environ. 324, 271–279. https://doi.org/10.1016/j.scitotenv.2003.10.034.
Foyer, C.H., Noctor, G., 2005. Redox homeostasis and antioxidant signaling: a metabolic interface between stress perception and physiological responses. Plant Cell 17, 1866–1875. https://doi.org/10.1105/tpc.105.033589.
Fu, S., Lu, Y., Zhang, X., Yang, G., Chao, D., Wang, Z., Shi, M., Chen, J., Chao, D.Y., Li, R., Ma, J.F., Xia, J., 2019. The ABC transporter *ABCG36* is required for cadmium tolerance in rice. J. Exp. Bot. 70, 5909–5918. https://doi.org/10.1093/jxb/erz335.
Greger, M., Wang, Y., Neuschütz, C., 2005. Absence of Hg transpiration by shoot after Hg uptake by roots of six terrestrial plant species. Environ. Pollut. 134, 201–208. https://doi.org/10.1016/j.envpol.2004.08.007.
Haque, S., Zeyaullah, M., Nabi, G., Srivastava, P.S., Ali, A., 2010. Transgenic tobacco plant expressing environmental E. coli merA gene for enhanced volatilization of ionic mercury. J. Microbiol. Biotechnol. 20, 917–924. https://doi.org/10.4014/jmb.1002.02001.
Hasan, M.K., Ahammed, G.J., Yin, L., Shi, K., Xia, X., Zhou, Y., Yu, J., Zhou, J., 2015. Melatonin mitigates cadmium phytotoxicity through modulation of phytochelatins biosynthesis, vacuolar sequestration, and antioxidant potential in *Solanum lycopersicum* L. Front. Plant Sci. 6, 601. https://doi.org/10.3389/fpls.2015.00601.
Huang, Y., Li, F., Yi, J., Yan, H., He, Z., Li, X., 2022. Transcriptomic and physio-biochemical features in rice (*Oryza sativa* L.) in response to mercury stress. Chemosphere 309, 136612. https://doi.org/10.1016/j.chemosphere.2022.136612.
Jang, J., Lee, O.R., 2020. Overexpression of ginseng patatin-related phospholipase pPLAIIIβ alters the polarity of cell growth and decreases lignin content in *Arabidopsis*. J. Ginseng Res. 44, 321e331. https://doi.org/10.1016/j.jgr.2019.01.004.
Jia, H., Wang, X., Wei, T., Xhou, R., Muhammad, H., Hua, L., Ren, X., Guo, J., Ding, Y., 2019. Accumulation and fixation of Cd by tomato cell wall pectin under Cd stress. Environ. Exp. Bot. 167, 103829. https://doi.org/10.1016/j.envexpbot.2019.103829.
Jung, H.I., Kong, M.S., Lee, B.R., Kim, T.H., Chae, M.J., Lee, E.J., Jung, G.B., Lee, C.H., Sung, J.K., Kim, Y.H., 2019. Exogenous glutathione increases arsenic translocation into shoots and alleviates arsenic-induced oxidative stress by sustaining ascorbate–glutathione homeostasis in rice seedlings. Front. Plant Sci. 10, 1089. https://doi.org/10.3389/fpls.2019.01089.
Kang, J., Park, J., Choi, H., Burla, B., Kretzschmar, T., Lee, Y., Martinoia, E., 2011. Plant ABC transporters. Arab. Book 9, e0153. https://doi.org/10.1199/table0153.
Kanwal, F., Tabusam, J., Khan, A., Askri, S.M.H., Ullah, S., Zhang, G., 2025. Zn induced Vmodifications in cell wall structure and lignin biosynthesis pathways improving cadmium tolerance in barley. Environ. Exp. Bot. 237, 106183. https://doi.org/10.1016/j.envexpbot.2025.106183.
Keunen, E., Remans, T., Bohler, S., Vangronsveld, J., Cuypers, A., 2011. Metal-induced oxidative stress and plant mitochondria. Int. J. Mol. Sci. 12, 6894–6918. https://doi.org/10.3390/ijms12106894.
Kim, Y.O., Bae, H.J., Cho, E., Kang, H., 2017. Exogenous glutathione enhances mercury tolerance by inhibiting mercury entry into plant cells. Front. Plant Sci. 8, 683. https://doi.org/10.3389/fpls.2017.00683.
Kim, Y.O., Gwon, Y., Kim, J., 2022. Exogenous cysteine improves mercury uptake and tolerance in *Arabidopsis* by regulating the expression of heavy metal chelators and antioxidative enzymes. Front. Plant Sci. 13, 898247. https://doi.org/10.3389/fpls.2022.898247.
Krzesłowska, M., Rabęda, I., Basińska, A., Lewandowski, M., Mellerowicz, E.J., Napieralska, A., Samardakiewicz, S., Woźny, A., 2016. Pectinous cell wall thickenings formation - A common defense strategy of plants to cope with Pb. Environ. Pollut. 214, 354–361. https://doi.org/10.1016/j.envpol.2016.04.019.
Lang, T., Hussain, M., Ishfaq, M., Shakoor, N., Tam, N.F.Y., Li, X., Pan, M., Zhu, Z., Xin, S., Zhou, H., 2025. Mercury-induced alterations in soil microbiome: A potential for microbiome stewardship to remediate contaminated soils. J. Clean. Prod. 512, 145717. https://doi.org/10.1016/j.jclepro.2025.145717.
Li, G.Z., Chen, S.J., Li, N.Y., Wang, Y.Y., Kang, G.Z., 2021. Exogenous glutathione alleviates cadmium toxicity in wheat by influencing the absorption and translocation of cadmium. Bull. Environ. Contam. Toxicol. 107, 320–326. https://doi.org/10.1007/s00128-021-03283-8.
Li, J., Yang, Z.L., Ding, T., Song, Y.J., Li, H.C., Li, D.Q., Chen, S., Xu, F., 2022. The role of surface functional groups of pectin and pectin-based materials on the adsorption of heavy metal ions and dyes. Carbohydr. Polym. 276, 118789. https://doi.org/10.1016/j.carbpol.2021.118789.
Li, L., Wu, W., Lin, H., Zhou, L., Zhang, D., Ishfaq, M., Zhong, Y., Li, B., Peng, Y., Wu, X., Yu, Y., Li, X., Chen, Q., 2024. Amino acid application inhibits root-to-shoot cadmium translocation in Chinese cabbage by modulating pectin methyl-esterification. Plant Physiol. Biochem 207, 108401. https://doi.org/10.1016/j.plaphy.2024.108401.
Li, R., Wu, H., Ding, J., Li, N., Fu, W., Gan, L., Li, Y., 2020. Transgenic *MerA* and *MerB* expression reduces mercury contamination in vegetables and grains grown in mercury-contaminated soil. Plant Cell. Rep. 39, 1369–1380. https://doi.org/10.1007/s00299-020-02570-8.
Liang, X., Ou, Y., Zhao, H., Qian, R., Sun, C., Lin, X., 2022. Short-chain aldehydes increase aluminum retention and sensitivity by enhancing cell wall polysaccharide contents and pectin demethylation in wheat seedlings. J. Hazard. Mater. 433, 128743. https://doi.org/10.1016/j.jhazmat.2022.128743.
Liu, T., Shen, C., Wang, Y., Huang, C., Shi, J., 2014. New insights into regulation of proteome and polysaccharide in cell wall of *Elsholtzia splendens* in response to copper stress. PLoS One 9, e109573. https://doi.org/10.1371/journal.pone.0109573.
Manara, A., 2012. Plant responses to heavy metal toxicity. Plants Heavy Met. 27–53. https://doi.org/10.1007/978-94-007-4441-7_2.
Manceau, A., Bustamante, P., Haouz, A., Bourdineaud, J.P., Gonzalez-Rey, M., Lemouchi, C., Gautier-Luneau, I., Geertsen, V., Barruet, E., Rovezzi, M., Glatzel, P., Pin, S., 2019. Mercury(II) binding to metallothionein in *Mytilus edulis* revealed by high energy-resolution XANES spectroscopy. Chemistry 25 9971009. https://doi.org/10.1002/chem.201804209.
Mao, C., Yi, K., Yang, L., Zheng, B., Wu, Y., Liu, F., Wu, P., 2004. Identification of aluminium-regulated genes by cDNA-AFLP in rice (*Oryza sativa* L.): aluminium-regulated genes for the metabolism of cell wall components. J. Exp. Bot. 55, 137–143. https://doi.org/10.1093/jxb/erh030.
Mendoza-Cózatl, D.G., Zhai, Z., Jobe, T.O., Akmakjian, G.Z., Song, W.Y., Limbo, O., Russell, M., Kozlovskyy, V.I., Martinoia, E., Vatamaniuk, O.K., Russell, P., Schroeder, J.I., 2010. Tonoplast-localized Abc2 transporter mediates phytochelatin accumulation in vacuoles and confers cadmium tolerance. J. Biol. Chem. 285, 40416–40426. https://doi.org/10.1074/jbc.M110.155408.
Mittler, R., Vanderauwera, S., Gollery, M., Van Breusegem, F., 2004. Reactive oxygen gene network of plants. Trends Plant Sci. 9, 490–498. https://doi.org/10.1016/j.tplants.2004.08.009.
Moons, A., 2003. *Ospdr9*, which encodes a PDR-type ABC transporter, is induced by heavy metals, hypoxic stress and redox perturbations in rice roots. FEBS Lett. 553, 370–376. https://doi.org/10.1016/S0014-5793(03)01060-3.
Moons, A., 2008. Transcriptional profiling of the PDR gene family in rice roots in response to plant growth regulators, redox perturbations and weak organic acid stresses. Planta 229, 53–71. https://doi.org/10.1007/s00425-008-0810-5.
Natasha, T., Shahid, M., Khalid, S., Bibi, I., Bundschuh, J., Niazi, N.K., Dumat, C., 2020. A critical review of mercury speciation, bioavailability, toxicity and detoxification in soil-plant environment: Ecotoxicology and health risk assessment. Sci. Total Environ. 711, 134749. https://doi.org/10.1016/j.scitotenv.2019.134749.
Oda, K., Otani, M., Uraguchi, S., Akihiro, T., Fujiwara, T., 2011. Rice *ABCG43* is Cd inducible and confers Cd tolerance on yeast. Biosci. Biotechnol. Biochem 75, 1211–1213. https://doi.org/10.1271/bbb.110193.
Park, J., Song, W.Y., Ko, D., Eom, Y., Hansen, T.H., Schiller, M., Lee, T.G., Martinoia, E., Lee, Y., 2012. The phytochelatin transporters AtABCC1 and AtABCC2 mediate tolerance to cadmium and mercury. Plant J. 69, 278–288. https://doi.org/10.1111/j.1365-313X.2011.04789.x.
Patra, M., Sharma, A., 2000. Mercury toxicity in plants. Bot. Rev. 66, 379–422. https://doi.org/10.1007/BF02868923.
Przedpelska-Wasowicz, E.M., Wierzbicka, M., 2011. Gating of aquaporins by heavy metals in *Allium cepa* L. epidermal cells. Protoplasma 248, 663–671. https://doi.org/10.1007/s00709-010-0222-9.
Roy, S.K., Naimuzzaman, M., Rahman, F., 2023. Glutathione: A key frontier of heavy-metal detoxification and tolerance in plants. Plant Trends 1, 33–42. https://doi.org/10.5455/pt.2023.05.
Rucińska-Sobkowiak, R., 2016. Water relations in plants subjected to heavy metal stresses. Acta Physiol. Plant 38, 257. https://doi.org/10.1007/s11738-016-2277-5.
Saha, J., Sengupta, A., Gupta, K., Gupta, B., 2015. Molecular phylogenetic study and expression analysis of ATP-binding cassette transporter gene family in *Oryza sativa* in response to salt stress. Comput. Biol. Chem. 54, 18–32. https://doi.org/10.1016/j.compbiolchem.2014.11.005.
Shao, R., Zhang, J., Shi, W., Wang, Y., Tang, Y., Liu, Z., Sun, W., Wang, H., Guo, J., Men, Y., Kang, G., Jagadish, K.S., Yang, Q., 2022. Mercury stress tolerance in wheat and maize is achieved by lignin accumulation controlled by nitric oxide. Environ. Pollut. 307, 119488. https://doi.org/10.1016/j.envpol.2022.119488.
Shivaraj, S.M., Deshmukh, R., Sonah, H., Bélanger, R.R., 2019. Identification and characterization of aquaporin genes in *Arachis duranensis* and *Arachis ipaensis* genomes, the diploid progenitors of peanut. BMC Genom. 20, 222. https://doi.org/10.1186/s12864-019-5606-4.
Song, W.Y., Park, J., Mendoza-Cózatl, D.G., Suter-Grotemeyer, M., Shim, D., Hörtensteiner, S., Geisler, M., Weder, B., Reae, P.A., Rentsch, D., Schroeder, J.I., Lee, Y., Martinoia, E., 2010. Arsenic tolerance in *Arabidopsis* is mediated by two ABCC-type phytochelatin transporters. Proc. Natl. Acad. Sci. U. S. A. 107, 21187–21192. https://doi.org/10.1073/pnas.1013964107.
Takeuchi, M., Watanabe, A., Tamura, M., Tsutsumi, Y., 2018. The gene expression analysis of Arabidopsis thaliana ABC transporters by real-time PCR for screening monolignol-transporter candidates. J. Wood Sci. 64, 477–484. https://doi.org/10.1007/s10086-018-1733-9.
Tang, Z., Fan, F., Deng, S., Wang, D., 2020. Mercury in rice paddy fields and how does some agricultural activities affect the translocation and transformation of mercury - A critical review. Ecotoxicol. Environ. Saf. 202, 110950. https://doi.org/10.1016/j.ecoenv.2020.110950.
Terzi, H., Yıldız, M., 2021. Proteomic analysis reveals the role of exogenous cysteine in alleviating chromium stress in maize seedlings. Ecotoxicol. Environ. Saf. 209, 111784. https://doi.org/10.1016/j.ecoenv.2020.111784.
Tian, J., Wang, L., Hui, S., Yang, D., He, Y., Yuan, M., 2023. Cadmium accumulation regulated by a rice heavy-metal importer is harmful for host plant and leaf bacteria. J. Adv. Res. 45, 43–57. https://doi.org/10.1016/j.jare.2022.05.010.
Truernit, E., Haseloff, J., 2008. A simple way to identify non-viable cells within living plant tissue using confocal microscopy. Plant Methods 4, 15. https://doi.org/10.1186/1746-4811-4-15.
Uraguchi, S., Sone, Y., Kamezawa, M., Tanabe, M., Hirakawa, M., Nakamura, R., Takanezawa, Y., Kiyono, M., 2019. Ectopic expression of a bacterial mercury transporter MerC in root epidermis for efficient mercury accumulation in shoots of

Arabidopsis plants. Sci. Rep. 9, 4347. https://doi.org/10.1038/s41598-019-40671-x.

Vats, S., Sudhakaran, S., Bhardwaj, A., Mandlik, R., Sharma, Y., Kumar, S., Tripath, D.K., Sonah, H., Sharma, T.R., Deshmukh, R., 2021. Targeting aquaporins to alleviate hazardous metal(loid)s imposed stress in plants. J. Hazard. Mater. 408, 124910. https://doi.org/10.1016/j.jhazmat.2020. 124910.

Vergilio, C.S., Carvalho, C.E.V., Melo, E.J.T., 2015. MercuryInduc. Dysfunct. Mult. Organe Lead. Cell death Vitro 29, 63–71. https://doi.org/10.1016/j.tiv.2014.09.006.

Voiniciuc, C., Pauly, M., Usadel, B., 2018. Monitoring polysaccharide dynamics in the plant cell wall. Plant Physiol. 176, 2590–2600. https://doi.org/10.1104/pp.17.01776.

Wang, F., Chen, F., Cai, Y., Zhang, G., Wu, F., 2011. Modulation of exogenous glutathione in ultrastructure and photosynthetic performance against Cd stress in the two barley genotypes differing in Cd tolerance. Biol. Trace Elem. Res. 144, 1275–1288. https://doi.org/10.1007/s12011-011-9121-y.

Xu, S., Sun, B., Wang, R., He, J., Xia, B., Xue, Y., Wang, R., 2017. Overexpression of a bacterial mercury transporter MerT in *Arabidopsis* enhances mercury tolerance. Biochem. Biophys. Res. Commun. 490, 528–534. https://doi.org/10.1016/j.bbrc.2017.06.073.

Yamamoto, S., Wasada, H., Kakitani, T., Yamato, T., 2001. Ab initio MO study on the potential energy surfaces for twisting around C15double bond N bond of protonated Schiff base of retinal. J. Mol. Struct. 543, 79–87. https://doi.org/10.1016/S0166-1280(00)00842-3.

Yang, L.P., Zhu, J., Wang, P., Zeng, J., Tan, R., Yang, Y.Z., Liu, Z.M., 2018. Effect of Cd on growth, physiological response, Cd subcellular distribution and chemical forms of *Koelreuteria paniculate*. Ecotoxicol. Environ. Saf. 160, 10–18. https://doi.org/10.1016/j.ecoenv.2018.05.026.

Yildiz, M., Terzi, H., 2021. Exogenous cysteine alleviates chromium stress via reducing its uptake and regulating proteome in roots of *Brassica napus* L. seedlings. S. Afr. J. Bot. 139, 114–121. https://doi.org/10.1016/j.sajb.2021.02.021.

Yu, L., Luo, Y., Liao, B., Xie, L., Chen, L., Xiao, S., Li, J.T., Hu, S.N., Shu, W.S., 2012. Comparative transcriptome analysis of transporters, phytohormone and lipid metabolism pathways in responseto arsenic stress in rice (*Oryza sativa*). N. Phytol. 195, 97–112. https://doi.org/10.1111/j.1469-8137.2012.04154.x.

Yuan, W., Wang, X., Lin, C.J., Wu, F., Luo, K., Zhang, H., Lu, Z., Feng, X., 2022. Mercury uptake, accumulation, and translocation in roots of subtropical forest: Implications of global mercury budget. Environ. Sci. Technol. 56, 14154–14165. https://doi.org/10.1021/acs.est.2c04217.

Zeng, F., Qiu, B., Wu, X., Niu, S., Wu, F., Zhang, G., 2012. Glutathione-mediated alleviation of chromium toxicity in rice plants. Biol. Trace Elem. Res. 148, 255–263. https://doi.org/10.1007/s12011-012-9362-4.

Zhang, Z., Chen, Y., Wang, D., Yu, D., Wu, C., 2023. Lignin-based adsorbents for heavy metals. Ind. Crops Prod. 193, 116119. https://doi.org/10.1016/j.indcrop.2022.116119.

Zhou, X., Xiong, X., Lu, F., Shi, W., Zhou, Y., Lai, N., Chen, L.S., Huang, Z.R., 2025. Excessive copper induces lignin biosynthesis in the leaves and roots of two citrus species: physiological, metabolomic and anatomical aspects. Ecotoxicol. Environ. Saf. 289, 117692. https://doi.org/10.1016/j.ecoenv.2025.117692.

Zhou, Z.S., Huang, S.Q., Guo, K., Mehta, S.K., Zhang, P.C., Yang, Z.M., 2007. Metabolic adaptations to mercury-induced oxidative stress in roots of *Medicago sativa* L. J. Inorg. Biochem 101, 1–9. https://doi.org/10.1016/j.jinorgbio.2006.05.011.